

People's Democratic Republic of Algeria
Ministry of Higher Education and Scientific Research
University M'Hamed BOUGARA – Boumerdes



Institute of Electrical and Electronic Engineering
Department of Electronics

Final Year Project Report Presented in Partial Fulfilment of the
Requirements for the Degree of

‘MASTER’

In Telecommunication
Option: Telecommunications

Title:

**Design and Analysis of a Dual-band Monopole
Antenna for Sub-6 GHz 5G Applications**

Presented By:

- **YAHOUI Yanes**
- **MOUSSAOUI Kamel**

Supervisor:

Dr M. DEHMAS

Registration Number:...../2023

Acknowledgement

First and foremost, we would like to praise and thank God, the almighty, who has granted countless blessings and provided me with the strength and guidance to complete this project. I am truly grateful for His unconditional and endless mercy, and grace. **Alhamdulillah.**

We would also like to express our gratitude to the people who have been instrumental in the successful completion of this project. Their support, encouragement, and guidance have been invaluable, and I am deeply grateful for their contributions.

We would like to thank our supervisor **Dr. M. DEHMAS** for his invaluable input, insights and assistance throughout the project. His expertise and guidance were instrumental in shaping the direction of this project.

We extend our sincere thanks to **Pr. AZRAR Arab, Pr. DAHIMENE** and **Pr. M. CHALLAL** for their constant guidance and encouragement during our curriculum as a telecommunication student.

Dedication

To our loving family,

You are our rock, our heart your unwavering love and support mean the world to us we cherish every memory we've created together. Thank you for always being there for us and for making our family a place of warmth and belonging.

To our dear friends,

You are the sunshine in our lives, the ones who lift us up and make every day brighter. Through the ups and downs, you've stood by our side, sharing laughter, and countless adventures

Thank you for being our chosen family and for filling our lives with love and laughter.

With heartfelt gratitude.

KAMEL and YANES

ABSTRACT

The project aims to design and analyze a microstrip slotted monopole antenna for sub-6 GHz 5G applications. The antenna is designed using symmetrical staircase and a ring slot. The proposed antenna is simulated using High Frequency Simulation Software (HFSS) to analyze its performance. The antenna exhibits a dual-band behavior. The first band extends from 2.3 to 4.9 GHz with a resonance at 3.5 GHz whereas the second band ranges from 5.3 to 7.2 GHz with a resonance at 6.6 GHz. The antenna is highly efficient with a maximum efficiency of about 97% and a peak gain of 3.4 dBi.

Based on the developed single patch, a 2x1 Multiple-Input Multiple-Output (MIMO) is developed. The obtained configuration provides qualitative Envelop Correlation Coefficient and diversity gain making it suitable for sub-6 GHz 5G applications.

Keywords: Monopole antenna; dual-band; MIMO; 5G.

Table of Contents

Acknowledgment.....	i
Dedication	ii
Abstract.....	iii
Table of contents.....	iv
List of Figures.....	vi
List of Tables.....	viii
List of Abbreviations.....	ix
General Introduction.....	1

Chapter 1: Antenna Basics and Microstrip Antennas.

1.1 Introduction.....	3
1.2 Microstrip antenna.....	3
1.3 Microstrip antenna characteristics.....	4
1.4 Feeding techniques.....	4
1.5 Fundamental parameters of antenna.....	6
1.5.1 Input reflection coefficient.....	6
1.5.2 Bandwidth.....	6
1.5.3 Directivity.....	7
1.5.4 Gain.....	7
1.6 Evolution of Wireless Communication System.....	7
1.6.1 Fifth Generation Wireless System.....	7
1.6.2 5G sub 6-GHz and microstrip antenna.....	8
1.7 Conclusion	9

Chapter 2: Design and Analysis of Dual-Band Monopole Antenna.

2.1 Introduction.....	10
2.2 Design and Geometry of the Proposed Dual-Band Antenna.....	10
2.2.1 Antenna design procedure and evolution	10
2.2.2 Current Distribution.....	17
2.2.3 Radiation Pattern	18

2.2.4 Gain and Efficiency.....	20
2.3 Experimental results.....	21
2.3.1 Input Reflection Coefficient.....	22
2.4 Comparison with related works.....	23
2.5 Conclusion.....	24

Chapter 3: Design and Simulation of a 2x1 MIMO Antennas.

3.1 Introduction	25
3.2 Dual-element MIMO antenna design procedure.....	25
3.2.1 Parallel configuration.....	25
3.2.2 Orthogonal polarization diversity configuration.....	33
3.3 Comparison between parallel and orthogonal configuration.....	38
3.4 Experimental Verification.....	39
3.5 Comparison with related works.....	41
3.6 Conclusion.....	42
General Conclusion and Further work	43

List of figures

Chapter 1: Antenna Basics and Microstrip Antennas.

Figure 1.1 Microstrip Patch Antenna Configuration.....	4
Figure 1.2 Classification of microstrip antenna feeding techniques.....	4
Figure 1.3 Microstrip Line Feed.....	5
Figure 1.4 Coaxial Probe Feed.....	5
Figure 1.5 Proximity Coupled Feed.....	5
Figure 1.6 Aperture coupled feed.....	6
Figure 1.7 The global 5G band spectrum.....	8

Chapter 2: Design and Analysis of Dual-Band Monopole Antenna.

Figure 2.1 Rectangular monopole antenna.....	11
Figure 2.2 Input Reflection coefficient magnitude versus Frequency.....	11
Figure 2.3 Symmetrical staircase patch antenna.....	12
Figure 2.4 Input reflection coefficient of symmetrical staircase antenna.....	14
Figure 2.5 Dual-band proposed antenna.....	15
Figure 2.6 Input reflection coefficient of the proposed antenna.....	17
Figure 2.7 Current Density Distribution.	18
Figure 2.8 The 2D radiation pattern, E plane and H plane.....	19
Figure 2.9 The 3D radiation pattern.....	20
Figure 2.10 Gain (dBi) versus frequency (GHz) of the proposed antenna.....	21
Figure 2.11 Radiation efficiency versus frequency of the proposed antenna.....	21
Figure 2.12 The fabricated antenna	22
Figure 2.13 The measured and simulated input reflection coefficients.....	23

Chapter 3: Design and Simulation of a 2x1 MIMO Antennas.

Figure 3.1 2×1 Parallel MIMO antenna.....	26
Figure 3.2 Input Reflection coefficient of Parallel MIMO antenna.....	26
Figure 3.3 Transmission coefficient of Parallel MIMO antenna.....	27
Figure 3.4 Envelope Correlation coefficient of the Parallel MIMO antenna.....	28
Figure 3.5 Diversity Gain of the MIMO antenna with Parallel configuration.....	28

Figure 3.6 Gain of MIMO antenna with Parallel configuration.....	29
Figure 3.7 Current density distribution of the MIMO antenna with Parallel configuration at 3.5 GHz.	30
Figure 3.8 Current density Distribution of the MIMO antenna with Parallel configuration at 6.6 GHz.	30
Figure 3.9 The 2D radiation pattern of the MIMO antenna with Parallel configuration, E plane and H plane.	31
Figure 3.10 The 3D radiation pattern of the MIMO antenna with Parallel configuration.	32
Figure 3.11 Proposed 2 × 1 MIMO for orthogonal polarization diversity.....	33
Figure 3.12 Input reflection coefficient at port 1 and port 2.....	33
Figure 3.13 Transmission coefficient of the Orthogonal MIMO antenna.....	34
Figure 3.14 Envelope Correlation coefficient of 2 × 1 MIMO system for orthogonal polarization diversity.	34
Figure 3.15 Diversity Gain of the MIMO antenna with orthogonal configuration.	35
Figure 3.16 Gain of MIMO antenna with orthogonal configuration	35
Figure 3.17 Current Density Distribution of the MIMO antenna with orthogonal configuration at 3.4 GHz.	36
Figure 3.18 Current Density Distribution of the MIMO antenna with orthogonal configuration at 6.4 GHz.	36
Figure 3.19 The 2D radiation pattern of the MIMO antenna with orthogonal configuration, E plane, and H plane.	37
Figure 3.20 The 3D radiation pattern of the MIMO antenna with orthogonal configuration. .	38
Figure 3.21 The front and the back view of 2x1 parallel fabricated MIMO antenna.	39
Figure 3.22 Input reflection coefficient at port 1.	40
Figure 3.23 Input reflection coefficient at port 2.	40
Figure 3.24 The transmission coefficient of the simulated and measured MIMO antenna.	41

List of Tables

Table 2.1 Effect of S1 on the performance of the antenna.....	13
Table 2.2 Effect of S2 on the performance of the antenna.....	13
Table 2.3 Effect of S3 on the performance of the antenna.....	13
Table 2.4 Effect of S4 on the performance of the antenna.....	14
Table 2.5 Input reflection coefficient magnitude and bandwidth for different values of d at the resonance of the second band.....	16
Table 2.6 Effects of the dimensions of the symmetrical stubs on the performance of the antenna.....	16
Table 2.7 The optimized dimensions of the proposed antenna.....	17
Table 2.8 Comparison between the simulated and the measured parameters of the staircase ring slotted monopole antenna.....	22
Table 2.9 Comparison with related works.....	23
Table 3.1 The results of the dual element MIMO antenna.....	32
Table 3.2 The results of the dual element MIMO with orthogonal configuration antenna.....	38
Table 3.3 Comparison with related works.....	41

List of Abbreviations

MIMO: Multiple-Input Multiple-Output

BW: Bandwidth

FR4: Flame Resistant 4

VSWR: Stands for Voltage Standing Wave Ratio

MPA: Microstrip patch antenna

RFID: Radio Frequency Identification

IoT: Internet of Things

RF: Radio frequency

QoS: Quality of service

NR: New radio

FR1: Frequency ranges 1

FR2: Frequency ranges 2

ECC: Envelope correlation coefficient

DG: Diversity gain

General Introduction

Nowadays, wireless communication is extensively used carrying information in different forms including voice, images and data. The magic of radio waves lies in the ability of antennas to detect and capture these vibrations from the air, and then convert them into usable data. Antennas are the key component that enables wireless devices to transmit and receive radio waves. A transmitting antenna takes signals from a transmission line and transforms them into electromagnetic waves, which are then broadcasted into the surrounding space. At the receiving end of the link, a receiving antenna collects these Electromagnetic waves and converts them back into their original signal form [1].

In high-performance aircraft, spacecraft, satellite, and missile applications, where size, weight, cost, performance, ease of installation, and aerodynamic profile are constraints, and low profile antennas may be required. To meet these requirements, microstrip antennas can be used [2-3].

Microstrip antennas in its simplest configuration consists of a radiating patch on one side of dielectric substrate ($\epsilon_r \leq 10$), which has a ground plane on other side [4].

The ever-growing demands for wireless communication face serious constraints on the 4th generation (4G) technology in terms of data-rate, bandwidth and delay. This has triggered the need for a 5th generation (5G) wireless communication technology which would not only provides a higher data-rate, large bandwidth, and lower delay, but also enable a variety of innovative applications such as self-driving cars, augmented reality and machine to machine communications. Fifth generation technology allows to provide faster internet speeds, lower latency and connect more devices simultaneously. Hence, It enables new applications that require high-bandwidth, low-latency connectivity [5].

Microstrip antennas offer several advantages for 5G applications including ability to provide directional radiation patterns, support of multiple-input multiple-output (MIMO) configurations. This makes microstrip antennas critical components in the development and deployment of 5G technology [6].

This project aims to propose a dual-band monopole antenna operating in frequency ranges

located in the Sub-6GHz frequency range allocated to 5G applications. This is obtained using a symmetrical star-case structure along with a slotted ring yielding a single element which is then used for development a MIMO configuration [7] .

This document includes three main chapters.

The first chapter discusses fundamentals of antenna parameters and microstrip structures.

The second chapter focuses on the design process of symmetrical staircase and ring slotted microstrip antennas. The chapter provides an in-depth discussion of the design steps taken to achieve performance from these antennas.

The third chapter provides a detailed insight into the development a MIMO structure based on the single element described in chapter 2.

Finally, the document ends up with a conclusion.

Chapter 1

Generalities on Microstrip Antennas

1.1 Introduction

Antennas are devices that are designed to transmit or receive electromagnetic waves. They are widely used in communication systems, including radio, television, mobile phones, and Wi-Fi. The antenna is the transitional structure between free-space and a guiding device. The guiding device or transmission line may take the form of a coaxial line or a hollow pipe (wave-guide), and it is used to transport electromagnetic energy from the transmitting source to the antenna, or from the antenna to the receiver. In the former case, we have a transmitting antenna and in the latter a receiving antenna [8].

Antennas come in many shapes and sizes, and the choice of antenna depends on the specific application. Some common types of antennas include dipole antennas, patch antennas, Yagi antennas, and helical antennas.

1.2 Microstrip Antenna

Throughout the evolution of wireless communication, antennas have captivated the attention of engineers, scientists, and wireless planners. Over the past few decades, antennas have undergone a significant transformation, transitioning from large dish-like structures to compact, foldable printed components found inside mobile phones and watches. As time progresses, the design and manufacturing of antennas have become increasingly convenient, thanks to the advent of Microstrip patch antennas [9].

The discovery and widespread adoption of microstrip patch antennas were driven by the need for compact, versatile, and cost-effective antenna solutions that could be seamlessly integrated into modern electronic systems. Their ability to offer miniaturization, integration flexibility, frequency range adaptability, directional control, and manufacturing ease made them a preferred choice over ground plane monopole antennas in the evolving landscape of wireless communications.

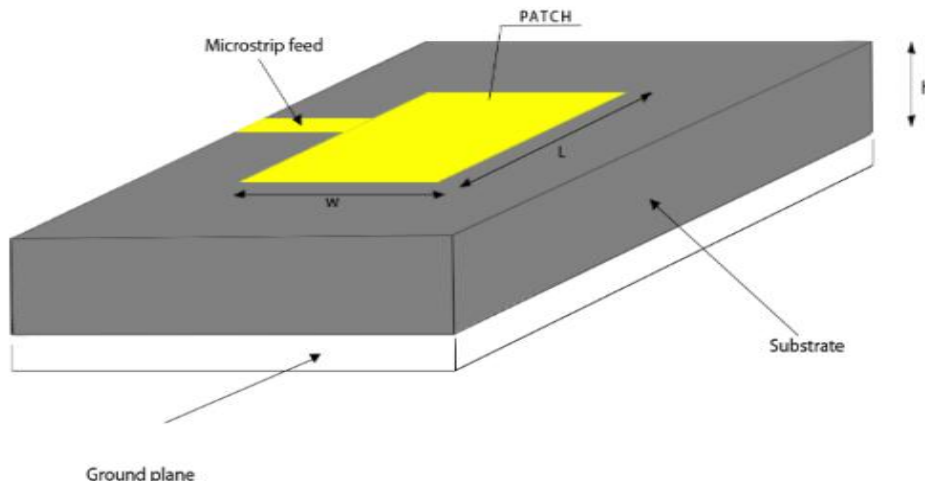


FIGURE 1.1 Microstrip Patch Antenna Configuration [10]

1.3 Microstrip Antenna Characteristics

A microstrip patch antenna (MPA) is a type of antenna that consists of a metallic patch printed on a grounded substrate. This configuration forms a microstrip transmission line structure. Patch antennas are known for their ease of design, simplicity of fabrication, and compact size, which has made them popular and widely used in wireless applications [11].

1.4 Feeding Techniques

Feeding techniques in antenna design refer to methods of delivering signals to the antenna. The most commonly used techniques can be classified into two primary groups: the contacting methods and the non-contacting methods, as shown in the figure 1.2.

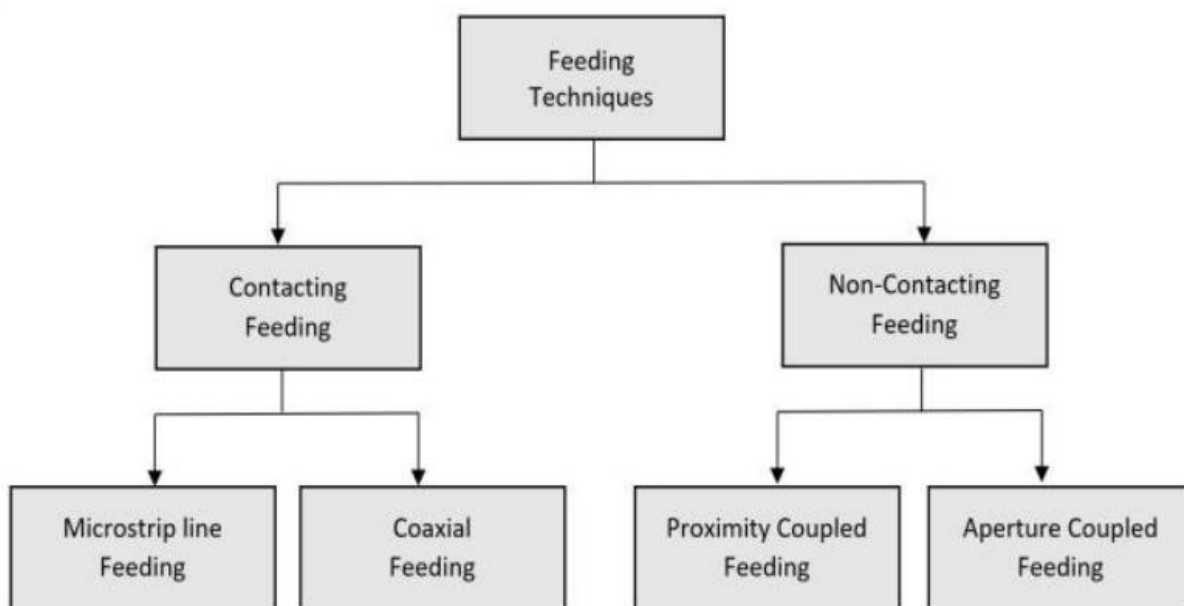


FIGURE 1.2 Classification of microstrip antenna feeding techniques [12]

The four different feeding techniques of MPA's are presented in the following figure:

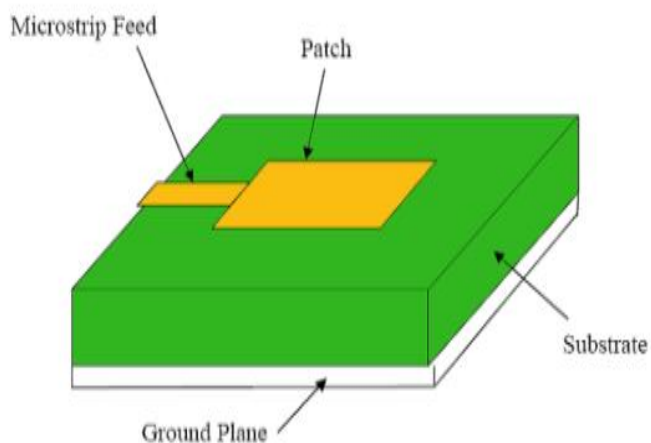


FIGURE 1.3 Microstrip Line Feed [13]

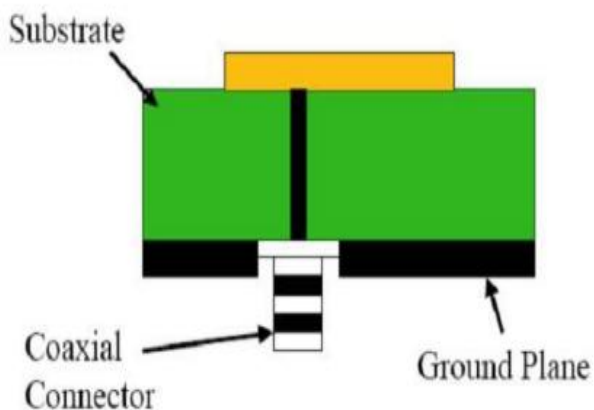


FIGURE 1.4 Coaxial Probe Feed [13]

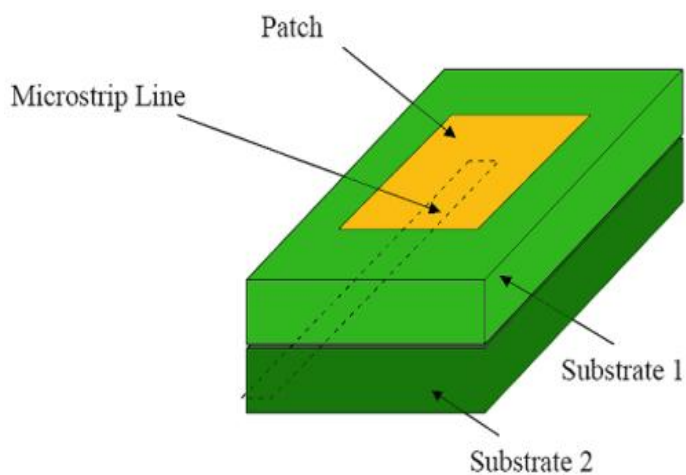


FIGURE 1.5 Proximity Coupled Feed [13]

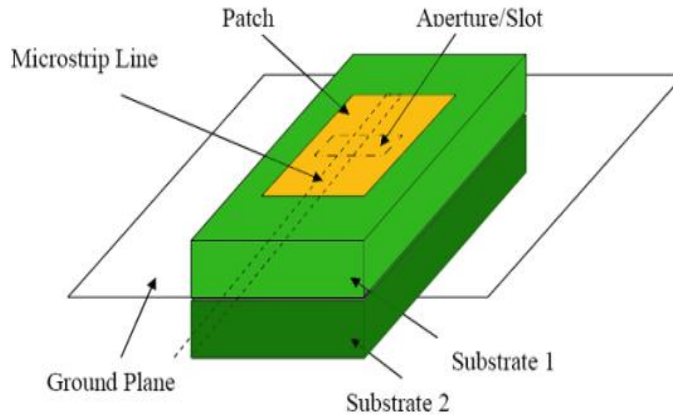


FIGURE 1.6 Aperture coupled feed [13]

1.5 Fundamental Parameters of an Antenna

There are several parameters that are used to describe the performance and characteristics of an antenna. These parameters are important for designing and optimizing antennas for specific applications and understanding them can help in selecting the right antenna for a particular use case, here are some of the basic antenna parameters:

1.5.1 Input Reflection Coefficient

Input reflection coefficient describes the amount of reflected power from an input device port with respect to the incident power. It is expressed in dB as:

$$|S_{11}|(dB) = 10 \log \left(\frac{p_r}{p_{in}} \right) = 20 \log \left| \frac{Z_{in} - Z_0}{Z_{in} + Z_0} \right| \quad (1.1)$$

Where: Z_{in} is the antenna input impedance.

Z_0 is the transmission line characteristic impedance.

P_{in} is the power supplied by the source and P_r denotes the reflected power.

1.5.2 Bandwidth

The bandwidth(BW) is a significant parameter for antennas, it is the antenna operating frequency band within which the antenna performs as desired. It is defined as the frequency range over which the magnitude of the input reflection coefficient remains below a certain threshold, typically -10 dB. In this definition, f_1 and f_2 represent the upper and lower frequency points, respectively, at which the reflection coefficient reaches -10 dB.

The equation is given as [14] :

$$BW \% = \frac{f_2 - f_1}{f_2 + f_1} \times 200 \quad (1.2)$$

1.5.3 Directivity: The directivity of an antenna is simply the measure of an antenna's ability to concentrate its radiated energy in a particular direction (ϕ, θ) . It is noted that the proposed formula provides a more accurate estimate of directivity than the geometrical mean formula [15].

The directivity of an antenna is defined as:

$$D(\theta, \phi) = \frac{U(\phi, \theta)}{U_0} = \frac{U(\phi, \theta)}{P_{rad}/4\pi} = \frac{4\pi U(\phi, \theta)}{P_{rad}} \quad (1.3)$$

1.5.4 Gain: Antenna gain determines the radiation pattern direction and the power transmitted or received in that direction, higher gains enhance wireless communication systems by improving range, coverage, and reliability.

The antenna gain $G(\theta, \phi)$, is related to the directivity via equation [16]:

$$G(\theta, \phi) = \frac{P_{rad}}{P_{in}} \times D(\theta, \phi) = e_T D(\theta, \phi) \quad (1.4)$$

e_T is the total efficiency given by [14]:

$$e_T = e_r (1 - |S_{11}|^2) \quad (1.5)$$

where e_r denotes the antenna radiation efficiency.

1.6 Evolution of Wireless Communication Systems

Nowadays, one of the fastest growing sectors in technology is wireless communication. Its increasing popularity stems from its ability to facilitate communication between multiple entities over any distance without the need for physical wires or cables. This communication is totally based on radio frequency (RF), With high speed data transmission rate. Wireless communication can be accessed from any location and at any time. That's why the modern world is running into the latest generation of technology, After crossing 1st to 4th generation, we are now in the era of 5th generation (5G) technology [17].

1.6.1 Fifth Generation Wireless System

Fifth Generation (5G) Technology is a recent generation of mobile networks. 5G provides a high data rate, improved quality of service (QoS), low-latency, high coverage, high reliability [18].

5G new radio (NR) supports operation in two frequency ranges: FR1 below 7,125 GHz which is known as Sub-6 GHz and mm Wave bands (FR2) between 24.25 and 52.6 GHz [19].

A sub-6 GHz (Mid band) has become the main focus of researchers due to the limitation of mm-waves. Since mm-waves are high-frequency waves, they can only cover very short range [20].

The figure bellow shows the band spectrum utilized in different countries:








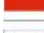


	<1 GHz	3 GHz	4 GHz	5 GHz	24-28 GHz	37-40 GHz	64-71 GHz
	600 MHz (2x35 MHz)	2.5/2.6 GHz (B41/n41)	3.45-3.55 GHz 3.7 GHz 4.2 GHz	5.9-7.1 GHz	24.25-24.45 GHz 24.75-25.25 GHz 27.5-28.35 GHz	37-37.6 GHz 37.6-40 GHz 47.2-48.2 GHz	64-71 GHz
	600 MHz (2x35 MHz)		3.55-3.7 GHz		26.5-27.5 GHz 27.5-28.35 GHz	37-37.6 GHz 37.6-40 GHz	64-71 GHz
	700 MHz (2x30 MHz)		3.4-3.8 GHz	5.9-6.4 GHz	24.5-27.5 GHz		
	700 MHz (2x30 MHz)		3.4-3.8 GHz		26 GHz		
	700 MHz (2x30 MHz)		3.4-3.8 GHz		26 GHz		
	700 MHz (2x30 MHz)		3.46-3.8 GHz		26 GHz		
	700 MHz (2x30 MHz)		3.6-3.8 GHz		26.5-27.5 GHz		
		2.5/2.6 GHz (B41/n41)	3.3-3.6 GHz	4.8-5 GHz	24.25-27.5 GHz	37-42.5 GHz	
			3.42-3.7 GHz		26.5-28.9 GHz		
			3.6-4.1 GHz	4.5-4.9 GHz 4.9 GHz	26.6-27 GHz 27-29.5 GHz	39-43.5 GHz	
			3.4-3.7 GHz		24.25-27.5 GHz	39 GHz	

FIGURE 1.7 The global 5G band spectrum [21]

1.6.2 5G sub 6-GHz and microstrip antenna

5G sub-6 GHz refers to the lower band frequencies used by 5G networks. Microstrip patch antennas are an optimal choice for 5G sub-6 GHz applications due to their low cost, lightweight, and compact design. The design of antennas for 5G operation in the sub-6 GHz frequency band significantly improves the performance as it leads to improve the overall system performance of the communication systems [22].

Several studies have proposed different microstrip patch antenna designs for 5G communication, including wide band microstrip patch antennas, high-gain wide band microstrip patch antennas, and patch antennas with enhanced gain and bandwidth. These antennas are designed to operate in the sub-6 GHz frequency range and are capable of providing wide band and high-gain performance. A low-profile rectangular slot antenna is

also suitable for sub-6 GHz 5G wireless applications. These antennas are essential for providing reliable and high-speed connectivity to 5G devices operating in the sub-6 GHz frequency range.

1.7 Conclusion

In this chapter, microstrip patch antennas were introduced along with feeding techniques. Antenna parameters such as gain, reflection coefficient and directivity take a huge amount of interest when analyzing the antenna performance.

Chapter 2

Design and Analysis of Dual-Band Monopole Antenna

2.1 Introduction

This chapter aims design and analysis of a single element dual-band monopole antenna suitable for wireless fifth generation applications in the sub-6 GHz frequency interval. As a rectangular patch structure is one of the basic investigated antenna geometries then a monopole antenna with a rectangular patch is initially considered and is taken as a reference design [23] . Modifications consisting on staircase geometry and a circular (ring) slot insertion are successively performed to end up with the final single element geometry.

The final symmetrical staircase and ring slotted antenna consists of staircase radiating element, 50-ohm feed line, partial ground with two symmetrical stubs, ring slot in the middle. The antenna is designed on an FR-4 substrate layer with $\epsilon_r = 4.4$, $\tan(\delta) = 0.02$ and a thickness (h) of 1.6 mm. The antenna dimensions are 30x20x1.6 mm³. The next section describes the achieved design steps and procedure using High Frequency Simulation Software (HFSS).

2.2 Design and Geometry of the Proposed Dual-Band Antenna

2.2.1 Antenna design procedure and evolution

2.2.1.1 Step-1 (Rectangular patch antenna)

Initially, a reference antenna consisting of a microstrip line fed rectangular patch antenna with a partial ground plane is used. The advantage of reducing the length of the ground plane is that it reduces capacitive coupling of the ground plane with the radiator, and hence, it helps to increase the bandwidth [24] .

In the first stage, the simple planar monopole antenna is taken as illustrated in figure 2.1 with the referenced dimension **Ls = 30mm, Ws = 20mm, Lp = 15.5mm, Lf = 13mm, Wf = 2mm** [25] .

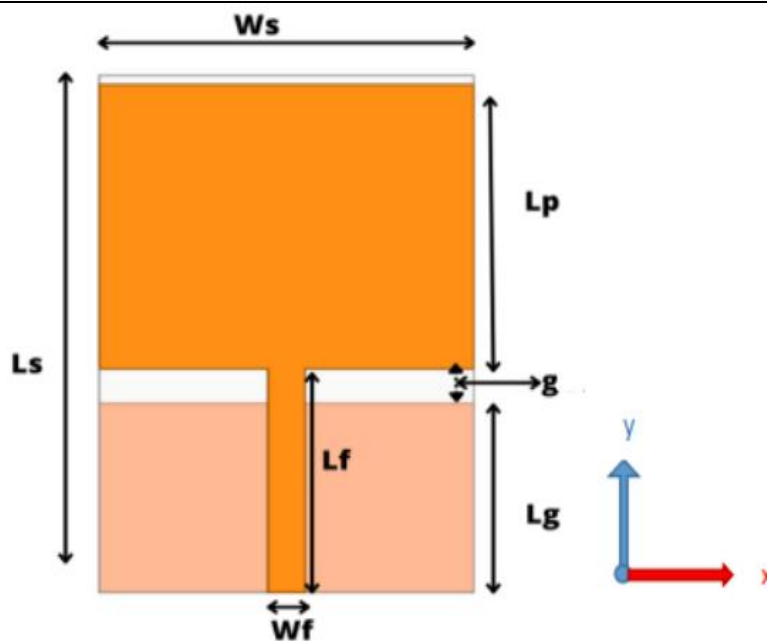


FIGURE 2.1 Rectangular monopole antenna

A. Effect of the gap between edges

First, the effect of the distance between the ground and the lower edge of the patch is investigated. To do that, a parametric study is carried out on the gap as illustrated in figure 2.2 which shows the input reflection coefficient for some gap (g) dimensions.

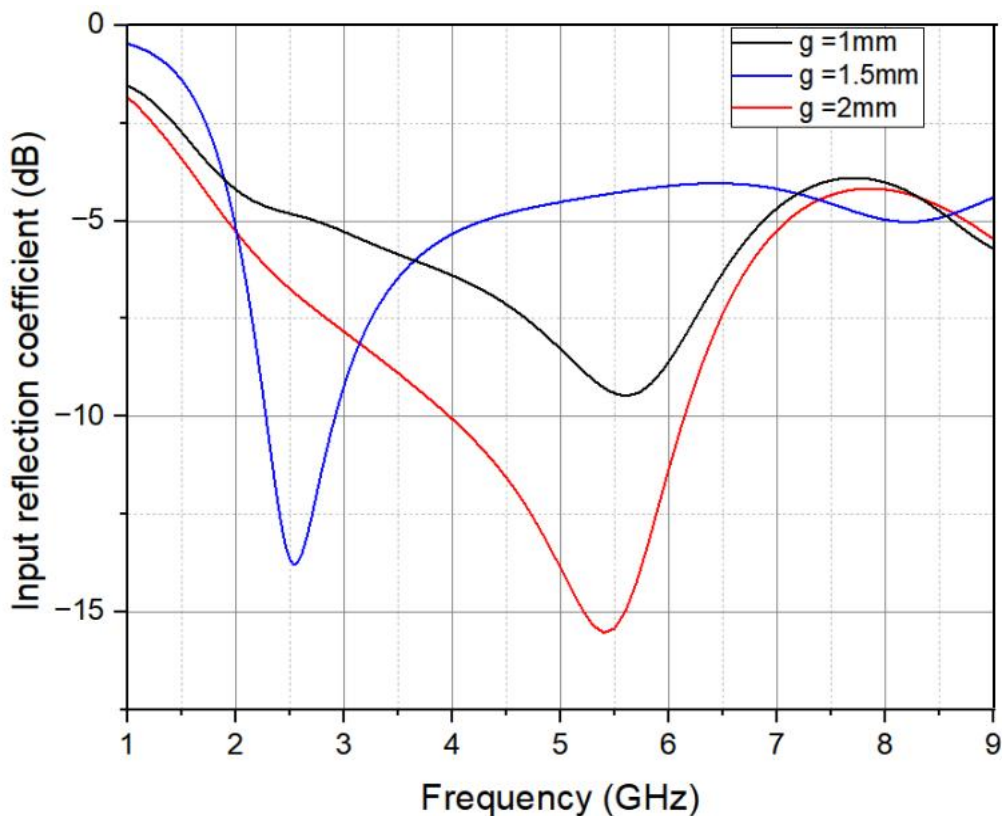


FIGURE 2.2 Input Reflection coefficient magnitude versus Frequency

This figure shows that a $g = 2 \text{ mm}$ gives the best results of bandwidth ($BW = 2.05 \text{ GHz}$) and impedance matching. We notice that the impedance bandwidth improvement comes from selecting a proper separation between the two edges.

2.2.1.2 Step-2 (Symmetrical staircase patch antenna)

In the second stage, two symmetrical staircases are inserted at the lower corners of the patch. Cutting L shapes at the corners of the patch increases separation from the patch to the ground plane.

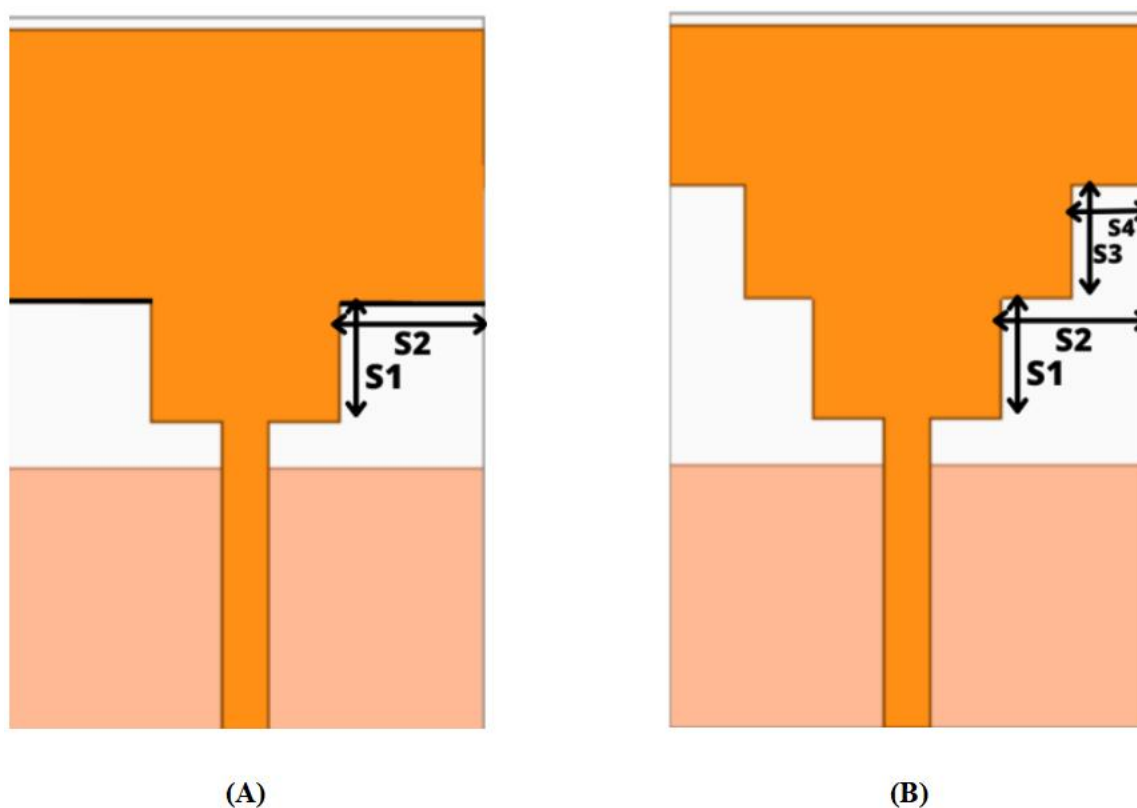


FIGURE 2.3 Symmetrical staircase patch antenna

The first rectangle is characterized by the dimensions $S1$ and $S2$, while the second rectangular has the dimensions $S3$ and $S4$ as shown in Figure 2.3. We perform a parametric study on each rectangular that shows their effect on the bandwidth and the impedance matching provided by this radiator.

A. Effect of the first rectangular dimensions $S1$ and $S2$

We vary $S1$ while the other dimension is fixed as: $S2 = 5.8 \text{ mm}$. The obtained results are illustrated in table 2.1.

TABLE 2.1 Effect of S1 on the performance of the antenna

S1 (mm)	5	5.2	5.4
 S₁₁ (dB) at 3.5 GHz	-15.3	-15.3	-15
BW(GHz)	2.05	1.9	2

The value **S1 = 5 mm** gives the best result in terms of bandwidth and impedance matching. Using the value **S1 = 5 mm** found from the previous parametric study the parameter **S2** is studied.

The obtained results are illustrated in table 2.2.

TABLE 2.2 Effect of S2 on the performance of the antenna

S2(mm)	5.6	5.8	6
 S₁₁ (dB) at 3.5 GHz	-14.72	-15.32	-16.6
BW(GHz)	1.9	1.95	2

It can be seen from Table 2.2 that the value **S2 = 6 mm** gives the best result of |S₁₁| in terms of bandwidth and impedance matching.

B. Effect of the second rectangular dimensions S3 and S4

We vary **S3** while the other dimension is fixed as: **S = 5.8 mm** the parameter S3 is studied.

The obtained results are illustrated numerically in table 2.3.

TABLE 2.3 Effect of S3 on the performance of the antenna

S3(mm)	4.6	4.8	5
 S₁₁ (dB)at 3.5 GHz	-15.6	-16.7	-16
BW(GHz)	2	2.1	2.1

It is noticed that the value **S3 = 4.8 mm** offers the best result in terms of bandwidth and impedance matching.

Using the value **S3 = 4.8 mm** obtained from the previous parametric study, the effect of the parameter S4 is studied.

The obtained results are illustrated numerically in table 2.4.

TABLE 2.4 Effect of S4 on the performance of the antenna

S4 (mm)	2.9	3.1	3.3
$ S_{11} $ (dB) at 3.5 GHz	-16.6	-17.3	-16.4
BW (GHz)	2.1	2.2	2

The value $S4 = 3.1 \text{ mm}$ gives the best result in terms of bandwidth and impedance matching. Figure 2.4 shows the input reflection coefficient of the antenna with the staircase dimensions: $S1 = 5 \text{ mm}$, $S2 = 6 \text{ mm}$, $S3 = 4.8 \text{ mm}$, $S3 = 3.1 \text{ mm}$, which generates two bands of operation. The first band with a bandwidth $BW = 2.2 \text{ GHz}$, the range of the band is $[2.2 \text{ GHz} - 4.7 \text{ GHz}]$ with a resonant frequency around 3.5 GHz which is suitable for 5G sub-6 GHz application. The second band need to be reduced to fit 5G sub-6 GHz operation. This is achieved in the next step by adding ring shaped slot [26-27].

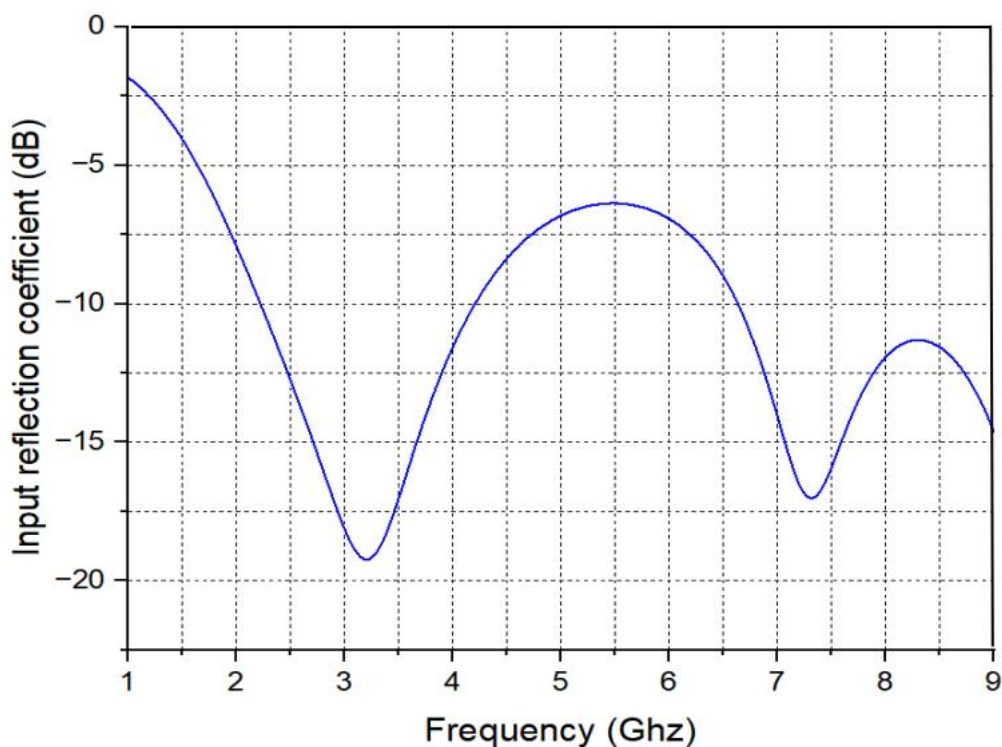


FIGURE 2.4 Input reflection coefficient of symmetrical staircase antenna

2.2.1.3 Step-3 (Proposed 5G Dual Band Antenna)

In this stage, a ring shaped slot with internal and external radii, $R1$ and $R2$, is inserted into the staircase patch as shown in Figure 2.5 to achieve a dual-band operation, fitting sub-6 GHz wireless 5G systems frequency band requirements [21].

Two symmetrical stubs are added to the ground plane to offer an inductance between the ground plane and patch, which neutralizes the capacitive and inductive effects to achieve a purely resistive impedance, hence a good impedance matching is provided with two bands of sub-6 GHz FR1 range [28] .

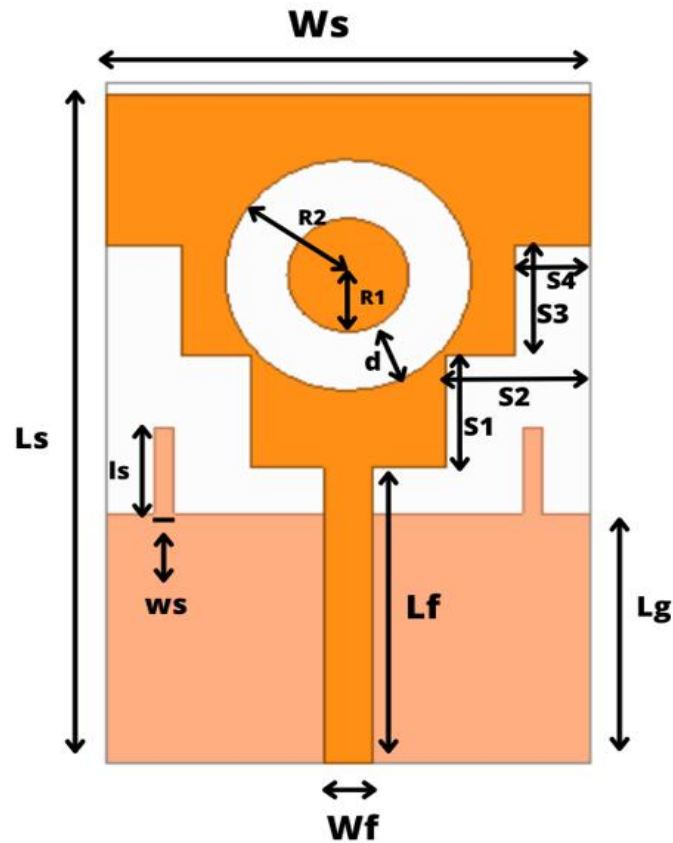


FIGURE 2.5 Dual-band proposed antenna

In order to optimize the dimensions of the ring slot which is described by the circles of radii R_1 and R_2 , we introduce the distance parameter between the two circles $d = R_2 - R_1$ where R_1 is fixed. The obtained results are illustrated numerically in Table 2.5 which displays the level of the input reflection coefficient ($|S_{11}|$ (dB)) for each value of the distance parameter d , and these values indicate appreciable matching of the patch at the second band.

TABLE 2.5 Input reflection coefficient magnitude and bandwidth for different values of **d** at the resonance of the second band

Radius 1 (R1) (mm)	2.5	2.5	2.5	2.5
Radius 2 (R2) (mm)	4.8	4.9	5.0	5.1
Distance d (mm)	2.3	2.4	2.5	2.6
 S₁₁ (dB) at 6.6 GHz	-18.86	-24.00	-27.00	-31.23
BW (GHz)	1.55	1.6	1.7	1.9

It is deduced from Table 2.5 that the value **d = 2.6 mm** gives the best results.

The design study is further extended, for purpose of accomplishment, to the dimensions **ls** and **ws** of the added symmetrical stubs to the ground. The results of this study are summarized in Table 2.6.

TABLE 2.6: Effects of the dimensions of the symmetrical stubs on the performance of the antenna

ws (mm)	0.8	0.8	0.8	0.8	0.8
ls (mm)	3	3.2	3.4	3.6	3.8
 S₁₁ (dB) at fr1= 3.5 (GHz)	-20.3	-20	-20	-20	-20.3
 S₁₁ (dB) at fr2= 6.6 (GHz)	-17.41	-20	-23	-27.66	-31.33
BW (%) of 1st band	65	65	67	68	74.28
BW (%) of 2nd band	20.9	22.42	24	25.45	28.33

The values **ws = 0.8 mm** and **ls = 3.8 mm** give the best result in terms of bandwidth and impedance matching.

The optimized dimensions of the proposed antenna are mentioned in table 2.7 below.

TABLE 2.7 The optimized dimensions of the proposed antenna

Parameters	Ls	Ws	Hs	Lp	Lf	Wf	R1
Values (mm)	30	20	1.6	15.5	20	2	2.5
Parameters	R2	S1	S2	S3	S4	ls	ws
Values (mm)	5.1	5	6	4.8	3.1	3.8	0.8

Figure 2.6 shows the input reflection coefficient of the proposed antenna where, the first band is [2.3 GHz - 4.9 GHz] with a bandwidth $BW = 2.6$ GHz and a resonant frequency $f_c = 3.5$ GHz, the second band [5.3 GHz - 7.2 GHz] with a bandwidth of $BW = 1.9$ GHz and a resonant frequency $f_c = 6.6$ GHz.

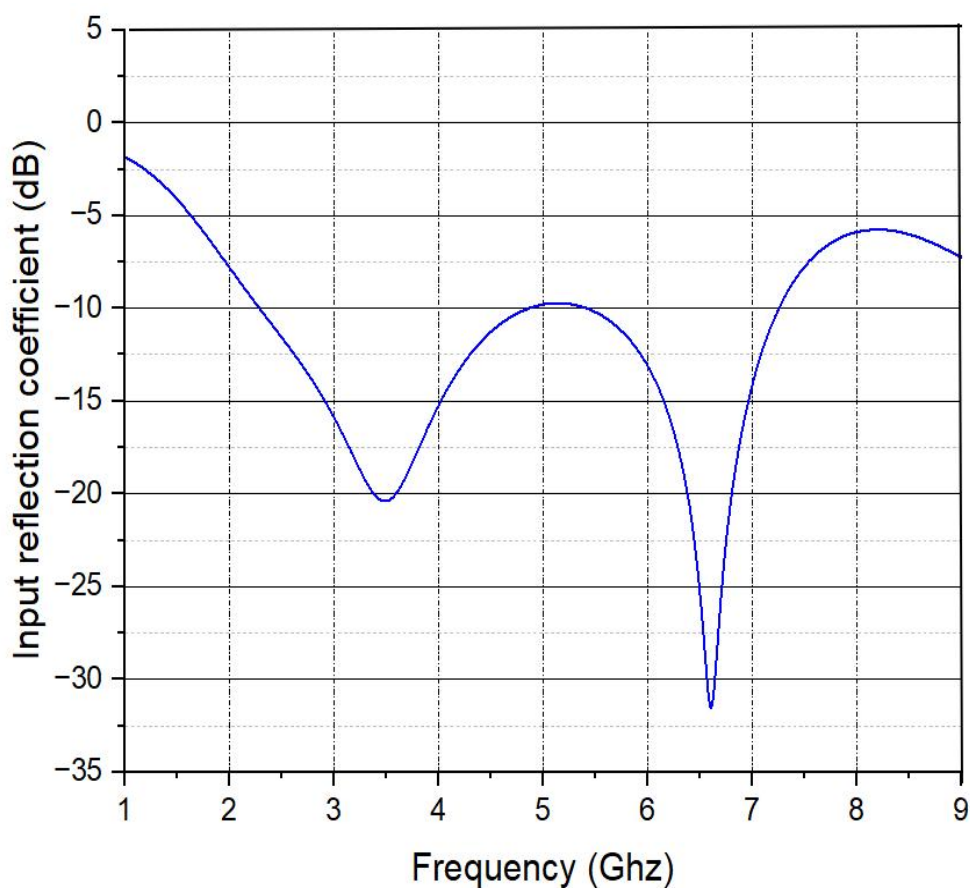


FIGURE 2.6 Input reflection coefficient of the proposed antenna

2.2.2 Current Density Distribution

Figure 2.7 depicts the current density distribution at two different frequencies, the frequencies were chosen to be the two resonant frequencies of the 1st and 2nd bands.

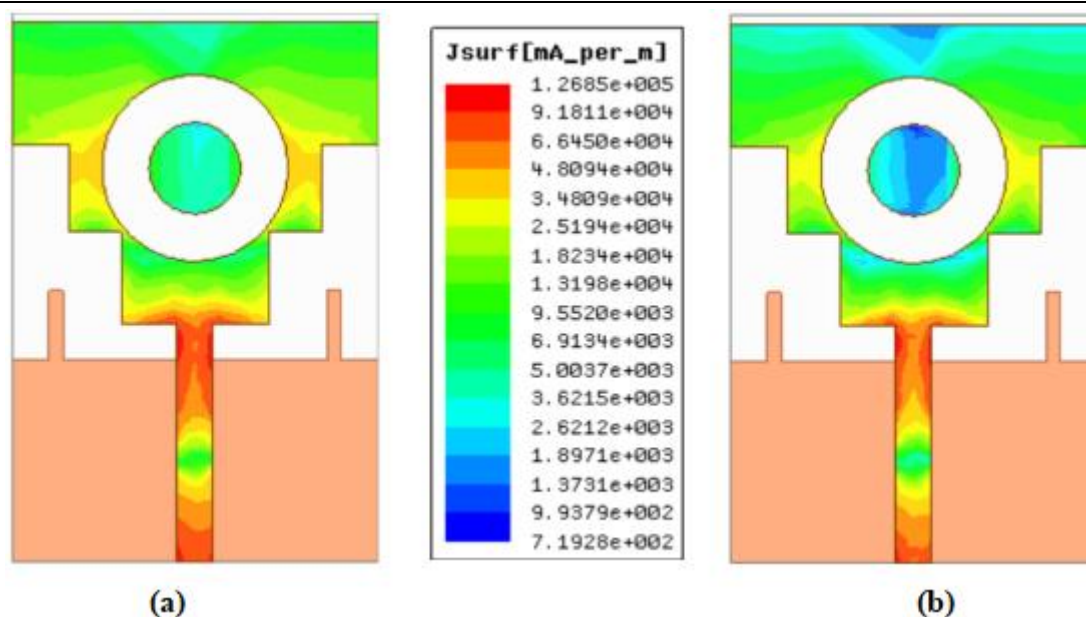


FIGURE 2.7 Current Distribution at a) 3.5 GHz, b) 6.6 GHz

It is seen from the figure 2.7 that the current density is mainly concentrated along the microstrip feeding line, around the ring slot and its center for the low resonance (3.5 GHz). As for the high resonance (6.6 GHz), it is also concentrated between the staircase structure and the ring slot.

2.2.3 Radiation Pattern

The directivity antenna is visualized in the 2D polar radiation pattern is shown in Figure 2.7.

At $f = 3.5$ GHz, the antenna exhibits a bidirectional pattern in the E-plane with a maximum directivity $D = 0.42$ dB at $\theta = 180^\circ$, and an omnidirectional pattern in the H-plane with a maximum directivity $D = 0.14$ dB at $\theta = 180^\circ$.

At $f = 6.6$ GHz, the antenna exhibits a bidirectional pattern in the E-plane with a maximum directivity $D = 2.77$ dB at $\theta = 350^\circ$, and an omnidirectional pattern in the H-plane with a maximum directivity $D = 2.73$ dB at $\theta = 0^\circ$

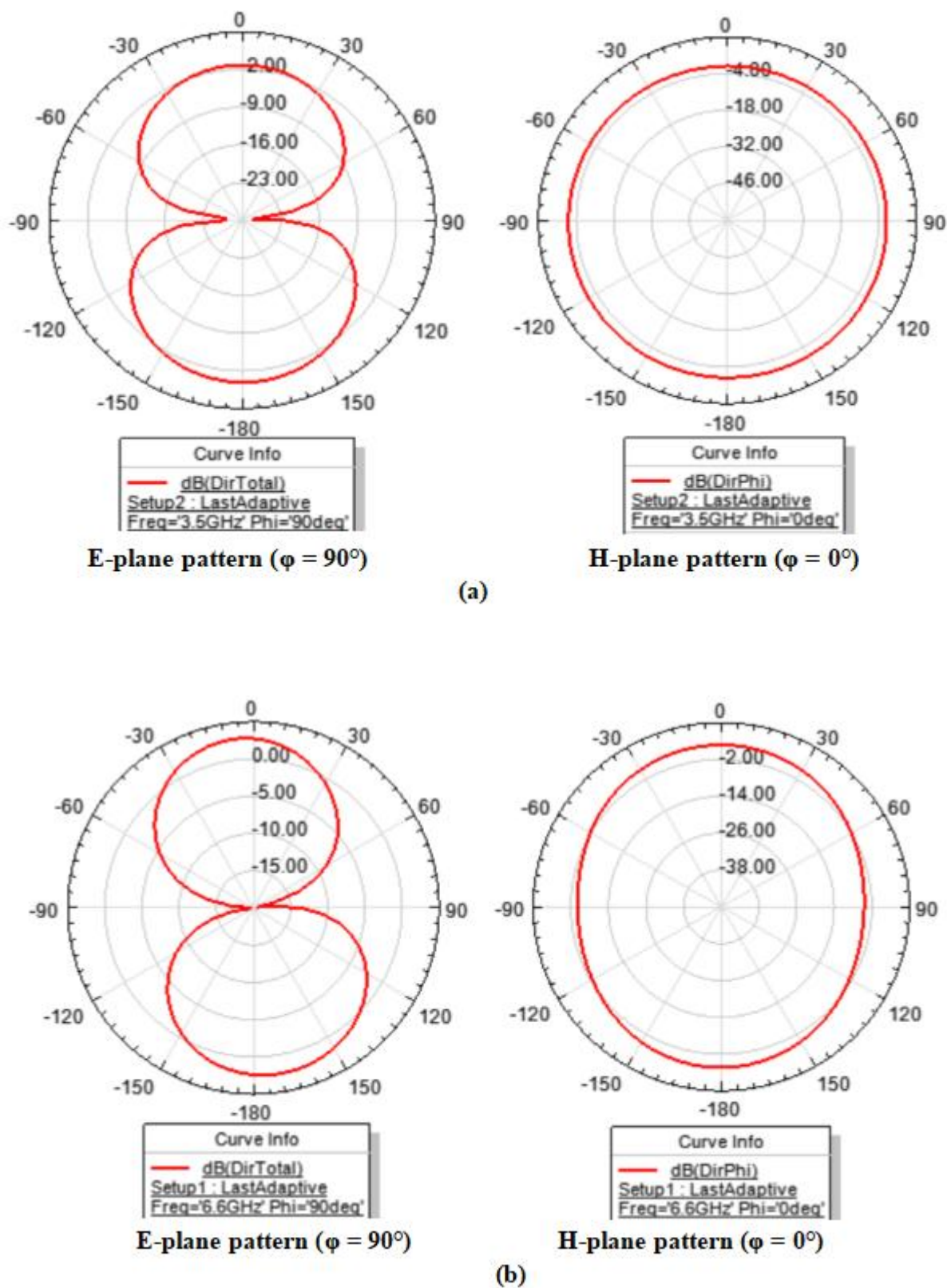


Figure 2.8 The 2D radiation pattern, E plane, and H plane at a) 3.5 GHz b) 6.6 GHz

Figure 2.9 represent the simulated 3D radiation pattern of the proposed antenna at frequencies 3.5 GHz and 6.6 GHz.

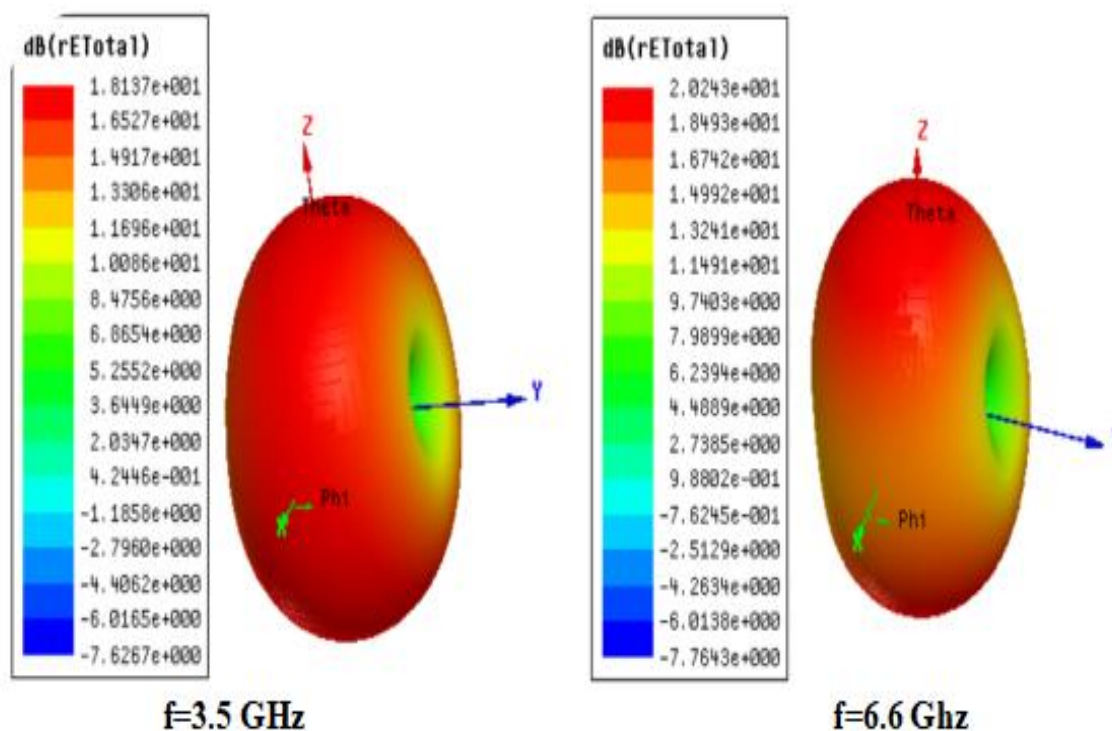


FIGURE 2.9 The 3D radiation pattern

2.2.4 Gain and Efficiency

The antenna peak gain and efficiency are illustrated in Figure 2.10 and Figure 2.11 respectively. The high gain and efficiency parameter values are attained in the sub-6 GHz band. The values of the gain at the two resonances are 1.1 dBi and 3.1 dBi respectively. The radiation efficiency of the antenna is around 96% over the range of operating frequencies, and its peak is obtained at the resonant frequency of the first band (3.5 GHz) with a value of -0.1 dB, so $10^{-0.01}$ which gives 0.9772 so the maximum efficiency is 97.72%. This is evidence that the symmetrical staircase with ring slot antenna has a good gain and efficiency values that contribute to its operation in 5G applications.

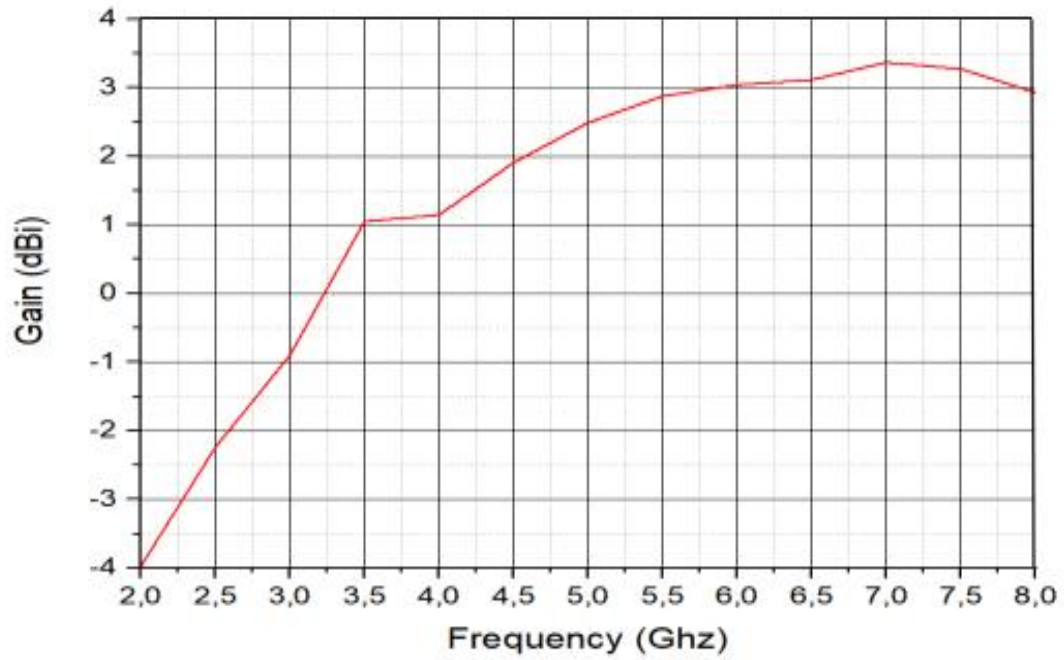


FIGURE 2.10 Gain (dBi) versus frequency (GHz) of the proposed antenna

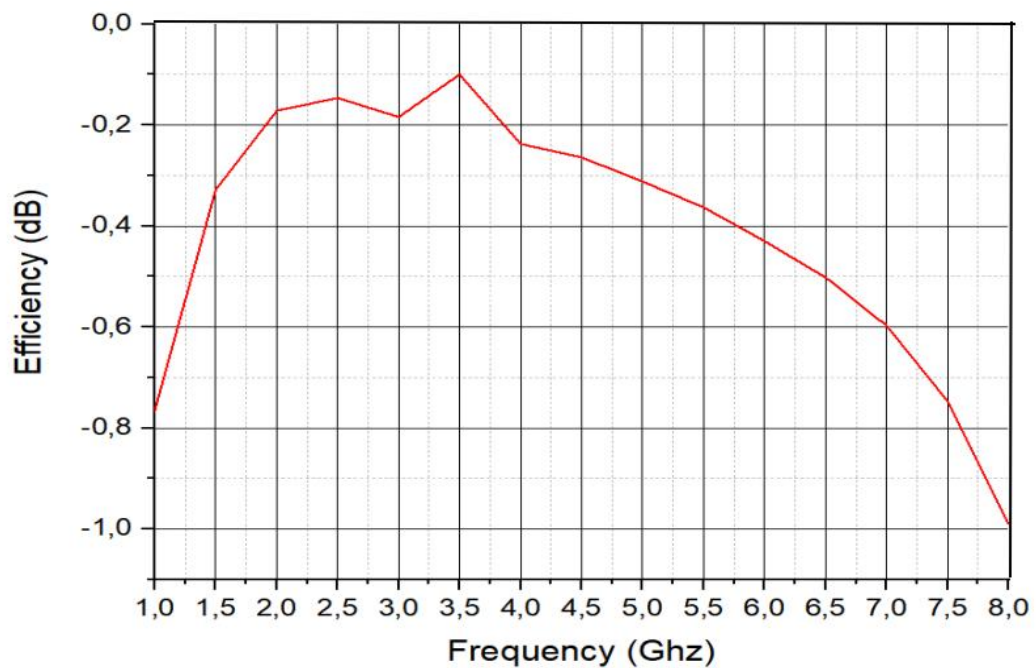


FIGURE 2.11 Radiation efficiency versus frequency of the proposed antenna

2.3 Experimental results

The proposed staircase monopole antenna is constructed in a private company (SNC ALMITech enterprise laboratory in Kouba ‘Algiers’). A photograph of the fabricated antenna is shown in Figure 2.12

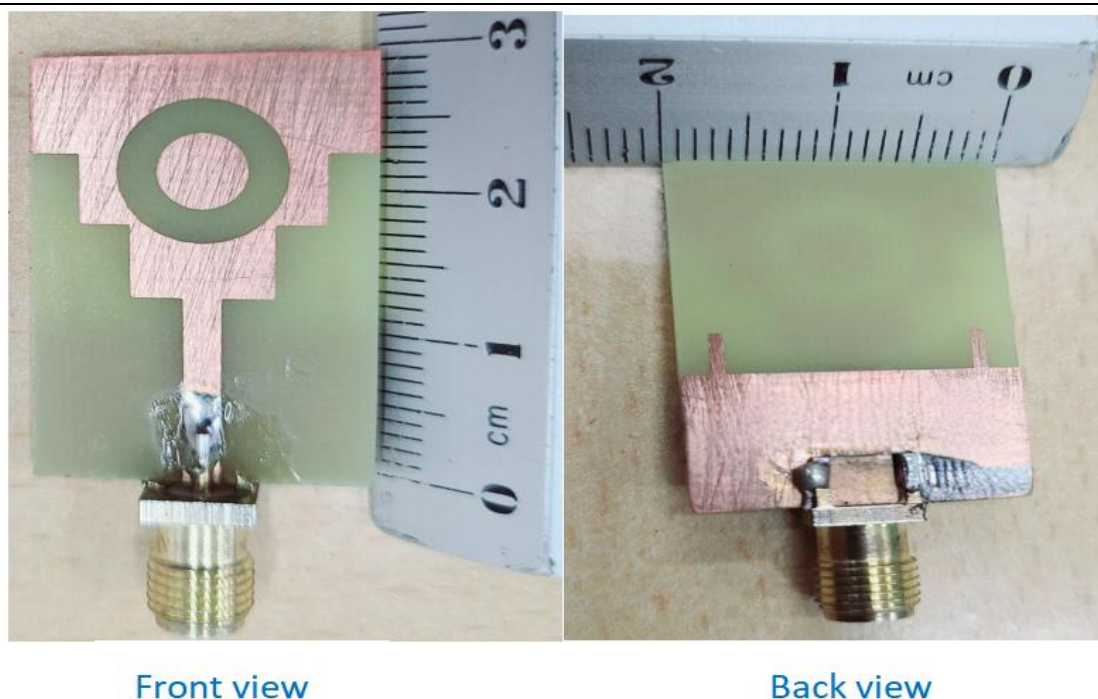


FIGURE 2.12 The fabricated antenna

2.3.1 Input Reflection Coefficient

The simulated and the measured reflection coefficient magnitude in dB of the proposed microstrip antenna is shown in Figure 2.13. The measured results confirm the dual band operation of the analyzed structure, however it can be observed that there are some deviations between simulated and measured. These deviations are due to several causes such as inaccuracies in the thickness and the dielectric permittivity of the fabricated substrate along with the experimental conditions. The differences are summarized in table 2.8.

TABLE 2.8 Comparison between the simulated and the measured parameters of the staircase ring slotted monopole antenna

Parameters	Simulated	Measured	Deviation
1 st resonant frequency	3.5 GHz	4.5 GHz	28.57 %
2 nd resonant frequency	6.6 GHz	7.5GHz	13.63 %
$ S_{11} $ at 3.5 GHz	-20.3 dB	-26 dB	28.07 %
$ S_{11} $ at 6.6 GHz	-31.33 dB	-45 dB	43.63%

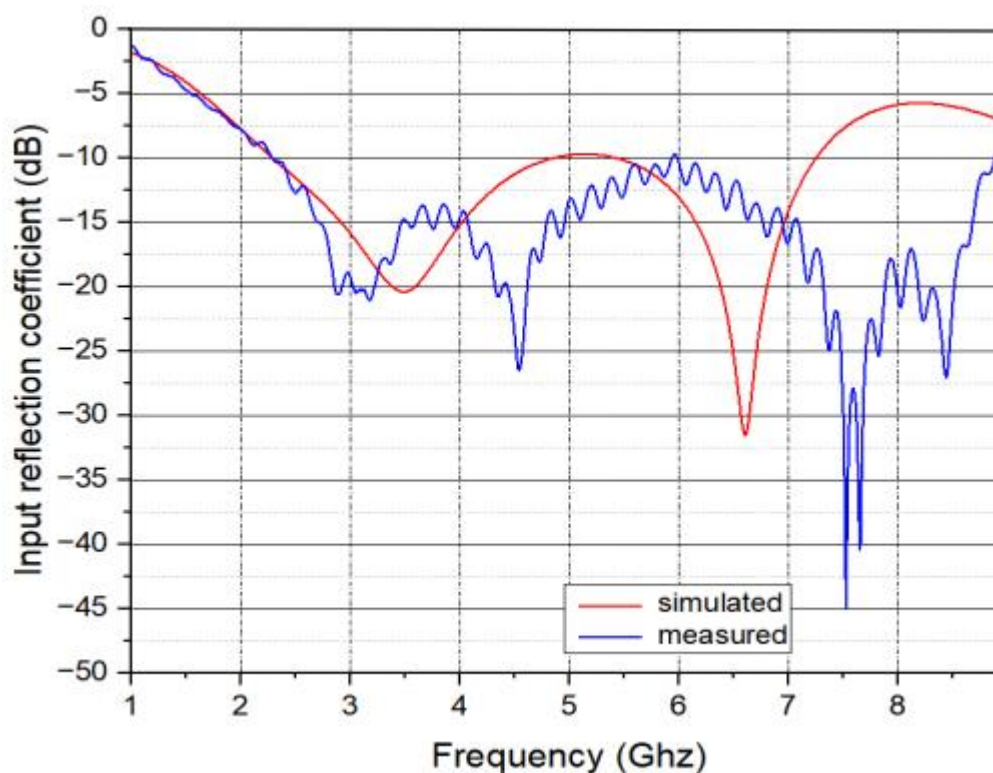


FIGURE 2.13 The measured and simulated input reflection coefficients

2.4 Comparison with related works

Table 2.9 shows a comparison between the proposed antenna characteristics with other works aiming similar objectives. These table shows that the proposed antenna exhibits acceptable performance especially dealing with gain, input reflection coefficient and efficiency

TABLE 2.9 Comparison with related works

References	[29]	[30]	[31]	Proposed antenna
Operating band (GHz)	3.11 - 3.82	3.23-4.27	3.12-3.22	2.30 - 4.91
	5.15 - 5.82	5.60-6.50	5.27-5.47	5.30-7.20
Dimensions (mm ³)	22 × 22 × 1.6	34 × 20 × 1	25.5 × 20 × 1.6	30 × 20 × 1.6
Peak Gain(dBi)	1.58	2.75	1.89	3.4
Efficiency (%)	92	95.8	85	97
Min S ₁₁ (dB) of 1 st band	-12	-20	-24.65	-20.3
Min S ₁₁ (dB) of 2 nd band	-26	-31	-18.04	-31.33

2.5 Conclusion

In this chapter, a single element monopole antenna has been designed and analyzed. The structure of the staircase with ring slotted antenna has dual-band operation of (2.3 GHz to 4.9 GHz) and (5.3 GHz to 7.2 GHz) which are suitable for 5G applications desired bands with a compact size.

Chapter 3

Design and Simulation of a 2x1 MIMO Antennas

3.1 Introduction

With the swift advancement of contemporary communication technologies, the multiple-input and multiple-output (MIMO) antenna systems have been progressively favored and extensively employed to acquire a substantial data transmission rate and expansive channel capacity. The primary drawback of the MIMO antenna is the mutual coupling between the radiating elements. In this chapter, the design of dual element MIMO antennas that are based on the symmetrical staircase and ring slotted antenna will be developed. The proposed design's evolution stages are also investigated. Furthermore, a parametric study is done on several parameters to get the accurate results to isolate the elements and keep them matched throughout the required 5G bands applications.

3.2 Dual-element MIMO antenna design procedure

The design is based on arranging two identical symmetrical staircase and ring slotted radiators on the top surface of the substrate, both parallel and orthogonal to each other. In the parallel configuration, the two elements are separated by a distance d of less than half-wavelength, because less than -20 dB of mutual coupling, and thus good isolation, can be easily achieved when the distance between radiators is larger than $\lambda/2$, but this does not meet the compactness requirement [32]. At the bottom, the antennas share the same partial ground plane with the same height as the single antenna.

3.2.1 Parallel configuration

Figure 3.1 shows the placement of the two radiators parallel to each other. To maintain the bandwidth performance and a good impedance matching in the two bands with a low mutual coupling while having a compact size, a parametric study is conducted on the distance d between the two patches.

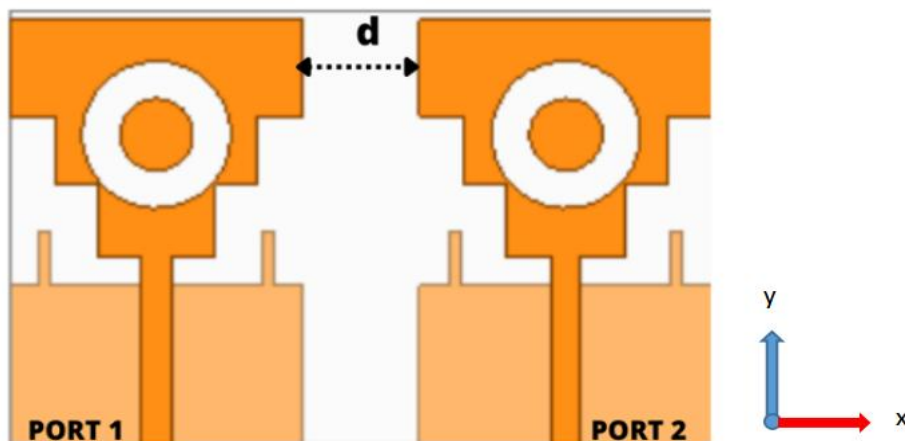


FIGURE 3.1 2×1 Parallel MIMO antenna

Figure 3.2 displays S-parameters of the parallel MIMO antenna at different distances

$d = 2\text{ mm} = \lambda_0/43$, $d = 7\text{ mm} = \lambda_0/12$ and $d = 10\text{ mm} = \lambda_0/5$. It is seen that the acceptable minimum edge-to-edge distance between the radiators is set to be 10 mm which is equivalent to $\lambda_0/9$ where the curve of the input reflection coefficient (S_{11}) at the two bands (2.3 GHz - 5 GHz) with BW = 2.7 GHz and (5.6 GHz-7.3GHz) with BW = 1.7 GHz indicates that the antenna is matched. The S_{12} is below -15 dB indicating that the antennas are isolated exclusively at all frequencies.

Remark: Since the elements are arranged symmetrically, the results for one port will be identical to those of the other one. For the sake of brevity, we will just simulate one port, observe and discuss it, while the same comments and observations are made about the other port.

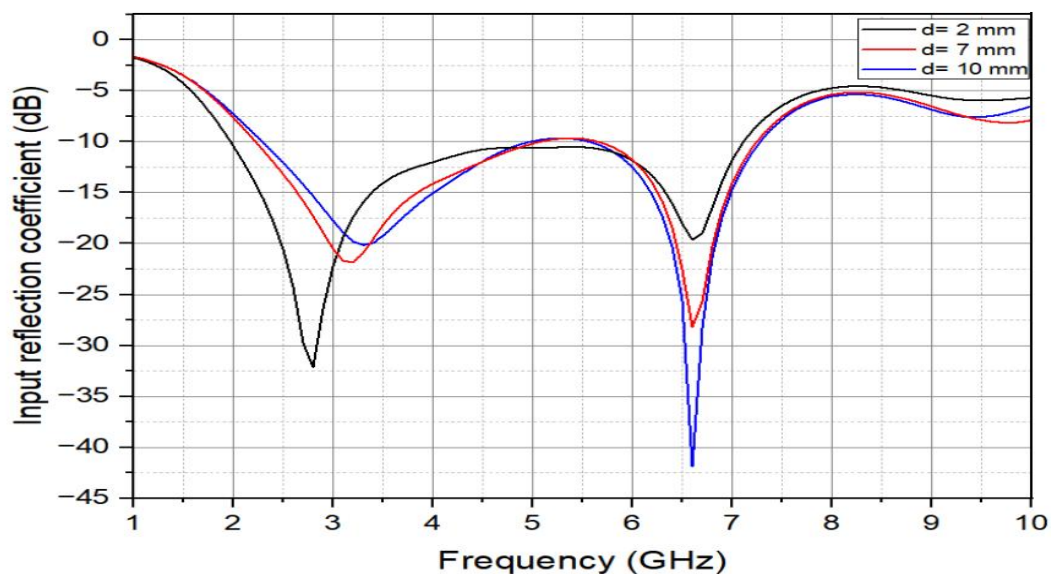


FIGURE 3.2 Input reflection coefficient of Parallel MIMO antenna at different spacing

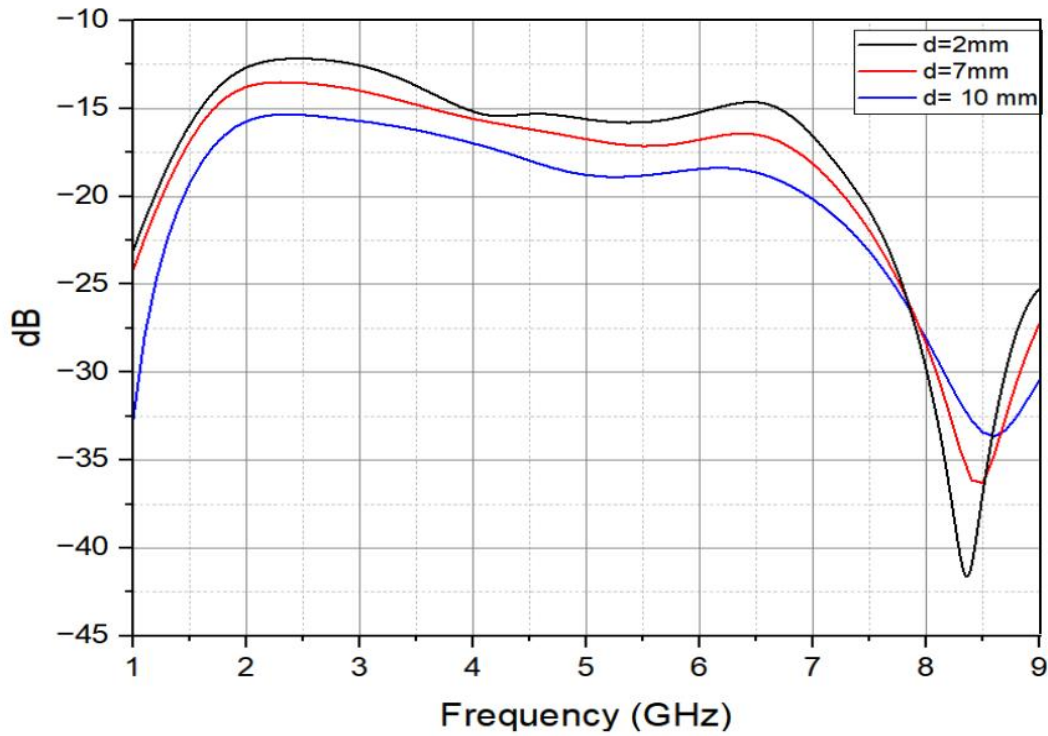


FIGURE 3.3 Transmission coefficient of Parallel MIMO antenna

3.2.1.1 Envelope correlation coefficient (ECC)

The degree of independence relating to the radiation patterns of two antennas is described with the help of ECC , the value of ECC must be minimum. The envelope correlation coefficient is calculated by equation (3.1) [33] .

$$ECC = \frac{|S_{11}S_{12}+S_{21}S_{22}|^2}{(1-(|S_{11}|^2+|S_{21}|^2))(1-(|S_{22}|^2+|S_{12}|^2))} \quad (3.1)$$

Through figure 3.3, it is evident that the value of ECC is below 0.075 over all frequencies, which can be considered a good envelope correlation coefficient. Concerning the operating band of the antenna the value of the ECC approaches zero at the resonances and is considerably low elsewhere.

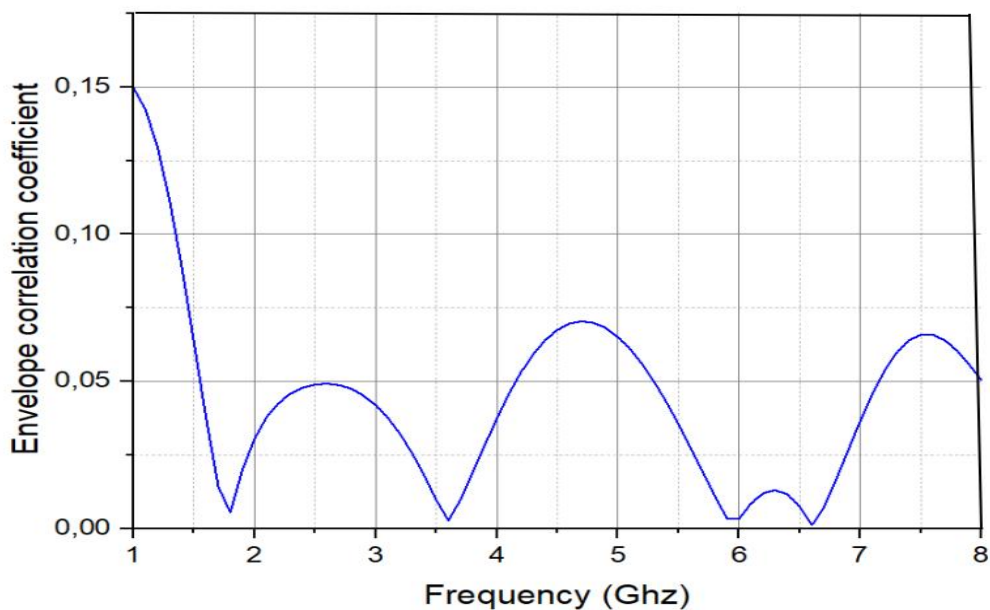


FIGURE 3.4 Envelope Correlation coefficient of the Parallel MIMO antenna

3.2.1.2 Diversity Gain

The diversity gain (DG) is a figure of merit used to quantify the performance level of diversity techniques. It is related to correlation coefficient by the equation [33] :

$$DG = 10(\sqrt{1 - |ECC|^2}) \quad (3.2)$$

The equation (3.2) shows that the lower the correlation coefficient the higher the diversity gain will be. Therefore, a high isolation is required between the antennas otherwise the DG will be low. For a satisfactory operation of MIMO antenna, DG should be close to 10 [30].

It is shown from Figure 3.5 that the diversity gain of MIMO antenna has values above 9.97 over the entire band

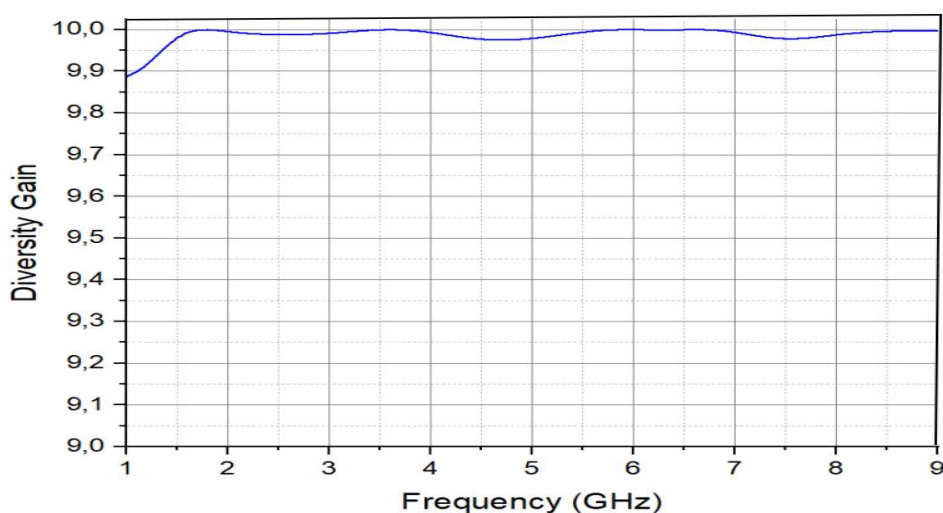


FIGURE 3.5 Diversity Gain of the MIMO antenna with Parallel configuration

3.2.1.3 Realized Gain

Figure 3.6 represents the parallel MIMO antenna's gain versus frequency. It is shown that the gain is enhanced as compared to the gain of the reference antenna (3.1 dBi) with a gain of 3.85 dBi.

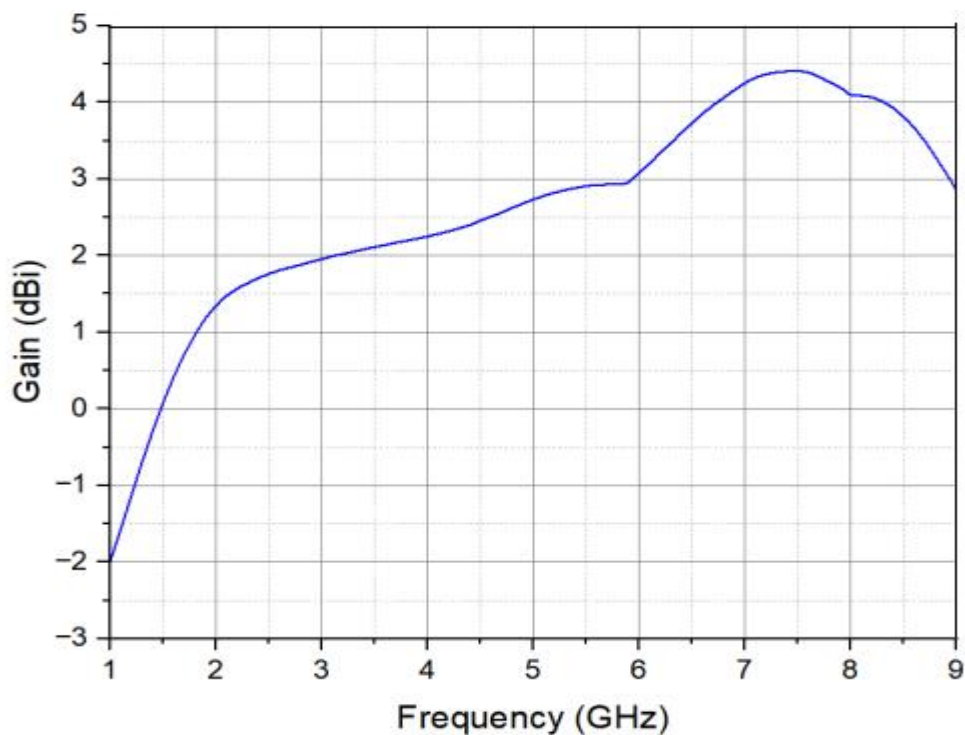


FIGURE 3.6 Gain of MIMO antenna with Parallel configuration

3.2.1.4 Current Density Distribution

The current density distribution on the two elements when exciting “port 1” at frequencies 3.5 and 6.6 GHz are illustrated in figure 3.7 and figure 3.8 respectively. This figure indicates clearly the current path involved in each of these frequencies. As expected, this path includes the main radiator length at both frequencies.

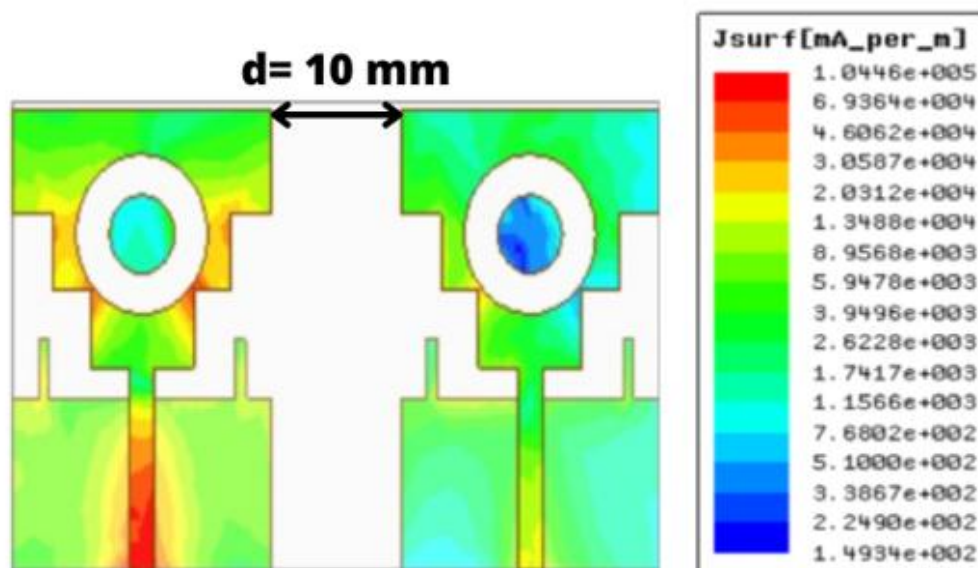


FIGURE 3.7 Current density distribution of the MIMO antenna with Parallel configuration at 3.5 GHz.

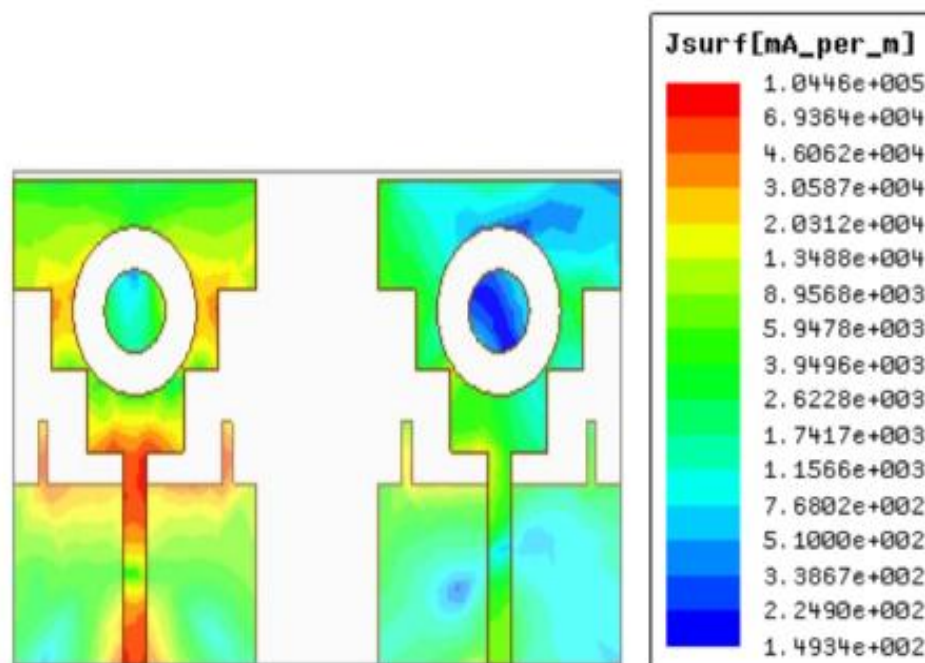


FIGURE 3.8 Current density distribution of the MIMO antenna with Parallel configuration at 6.6 GHz.

3.2.1.5 Radiation Pattern

The directivity of the two element MIMO antenna is visualized in the 2D polar radiation pattern at port 1 shown in Figure 3.9.

At $f = 3.5 \text{ GHz}$, the antenna exhibits a bidirectional pattern in the E-plane with a maximum directivity $D = 0.59 \text{ dB}$ at $\theta = 155^\circ$, and an omnidirectional pattern in the H-plane with a

maximum directivity $D = 1.31$ dB at $\theta = 205^\circ$.

At $f = 6.6$ GHz, the antenna exhibits a bidirectional pattern in the E-plane with a maximum directivity $D = 4.12$ dB at $\theta = 350^\circ$, and an omnidirectional pattern in the H-plane with a maximum directivity $D = 3.65$ dB at $\theta = 0^\circ$.

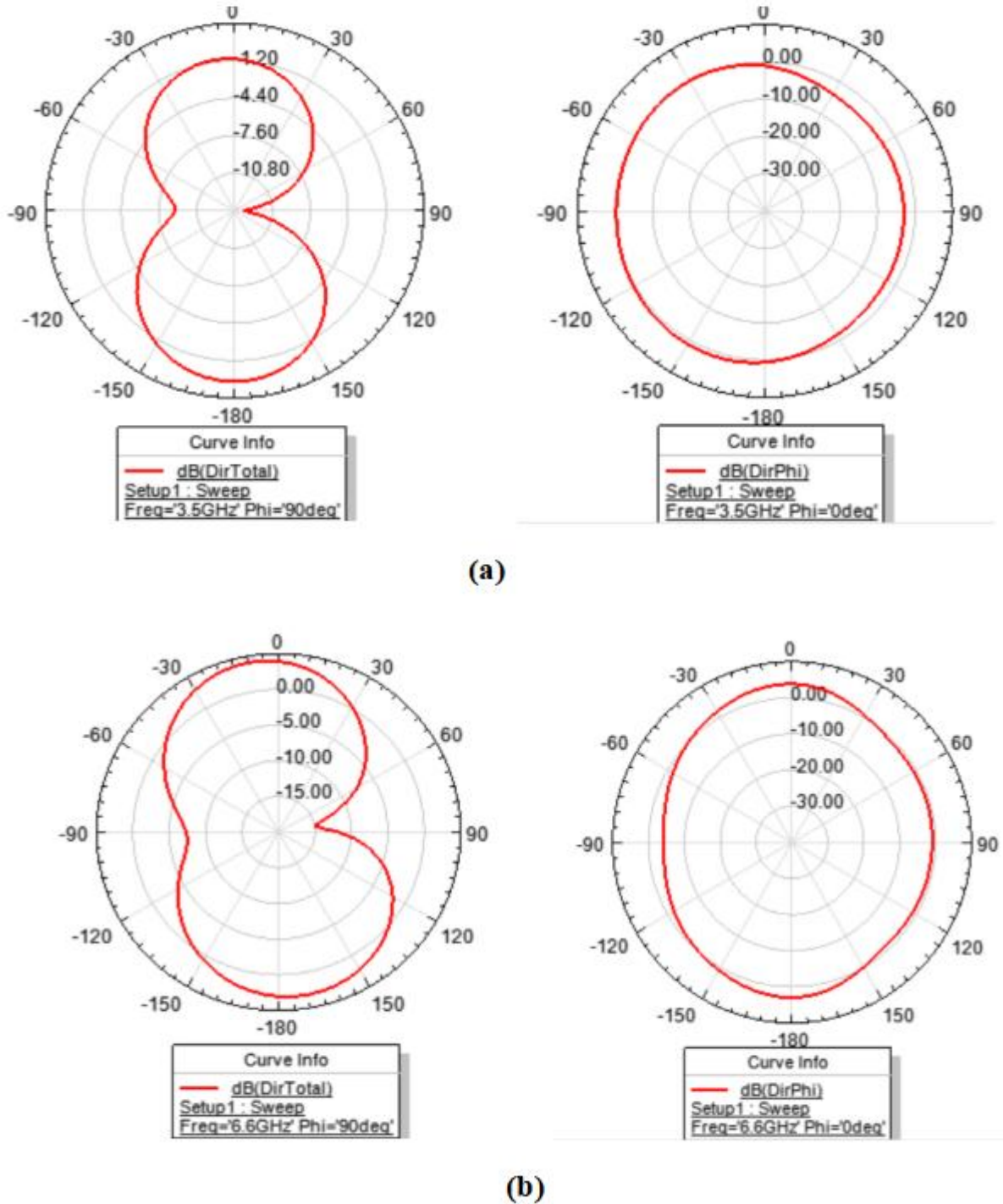


Figure 3.9 The 2D radiation pattern of the MIMO antenna with Parallel configuration, E plane and H plane at a) 3.5 GHz, b) 6.6 GHz

Figure 3.10 demonstrate the 3D radiation pattern of the two element MIMO antenna.

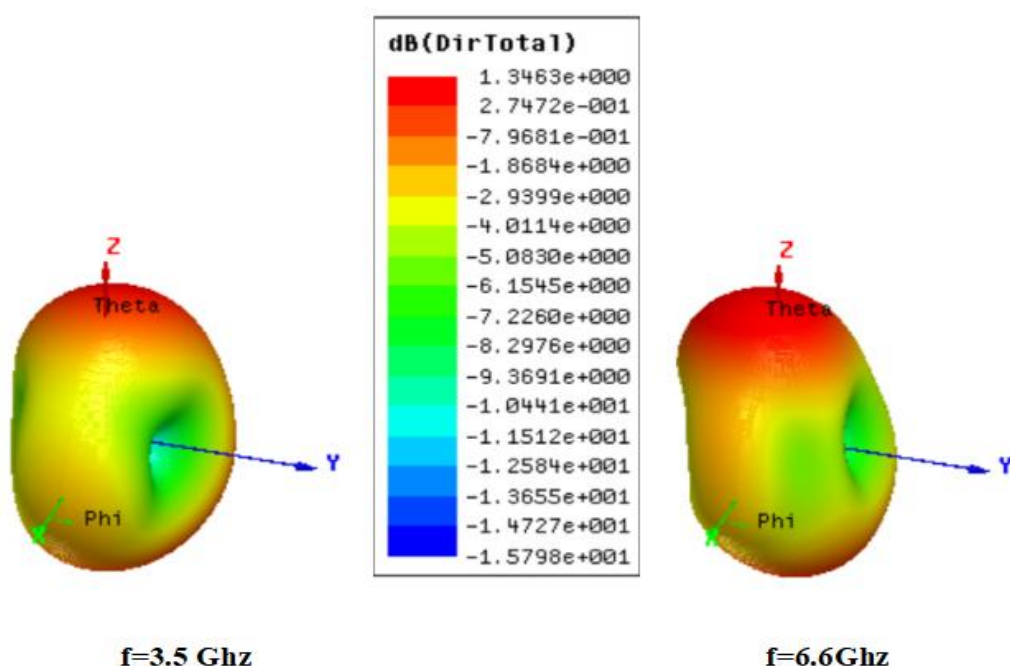


Figure 3.10 The 3D radiation pattern of the MIMO antenna with Parallel configuration

Table 3.1 summarizes the results in details of the dual element MIMO antenna.

TABLE 3.1 The results of the MIMO antenna with Parallel configuration

Number of elements	2
Size (mm^3)	$50 \times 30 \times 1.6$
Materials	FR-4 ($\epsilon_r = 4.4$)
Bandwidth of 1 st band (GHz)	2.9
Bandwidth of 2 nd band (GHz)	1.7
Isolation (dB)	-15.5
ECC	<0.075
DG (dB)	>9.97
Peak Gain (dB)	4.49

3.2.2 Orthogonal polarization diversity configuration

Figure 3.11 depicts the orthogonal configuration of the two-element antennas.

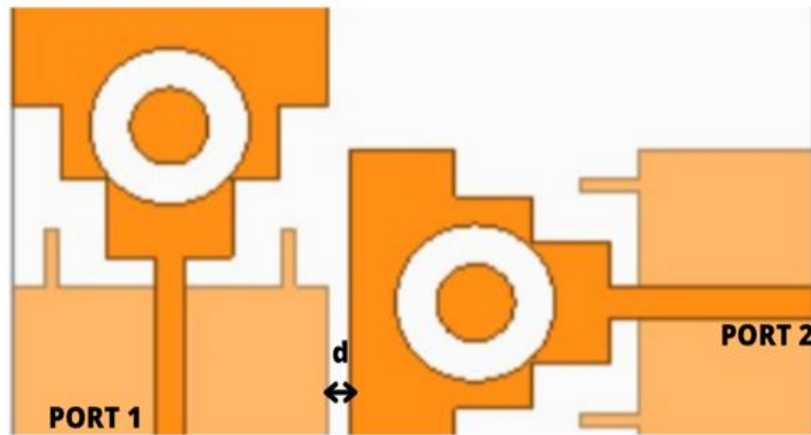


FIGURE 3.11 Proposed 2×1 MIMO for orthogonal polarization diversity

It can be inferred from Figure 3.12 that while the input reflection coefficient at port 1 (S_{11}) produces a dual-band characteristic extending from 2.4 GHz to 4.3 GHz with a resonant frequency $f_c = 3.4$ GHz and from 5.6 GHz to 7.25 GHz with $f_c = 6.4$ GHz, the input reflection coefficient at port 2 (S_{22}) produces a wide band characteristics extending from 2.2 GHz to 7.4 GHz. One can observe from Figure 3.13 that the antennas are already isolated over the whole band with an edge-to-edge distance of $d = 1$ mm only.

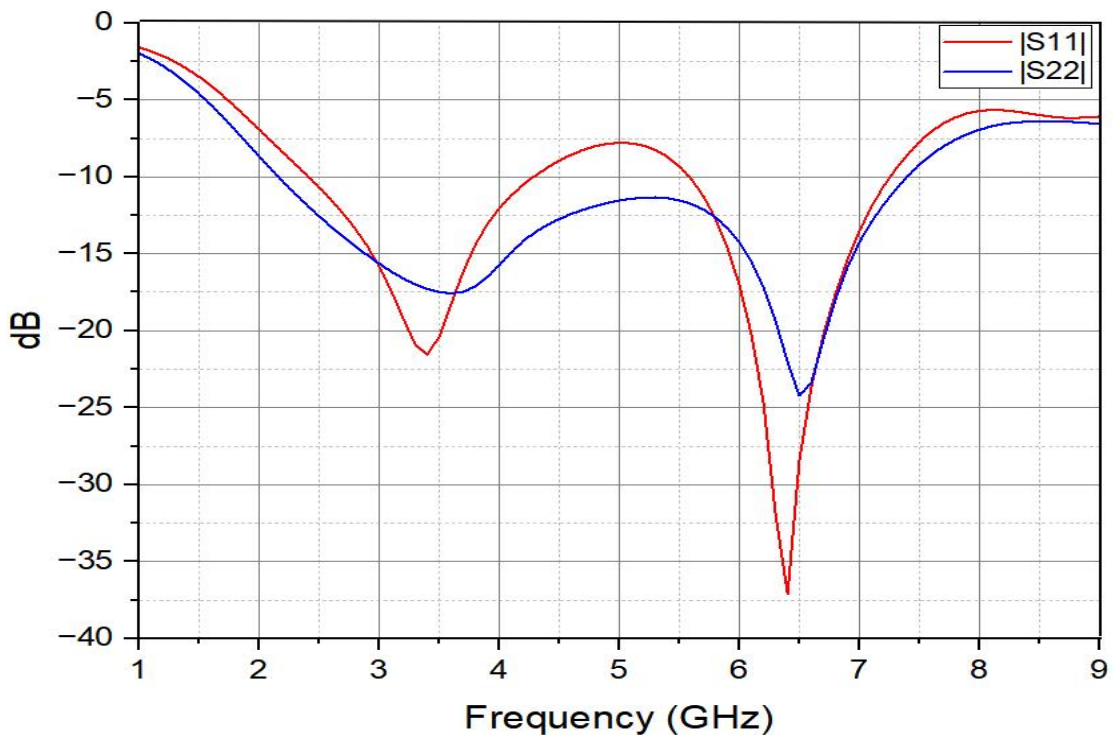


FIGURE 3.12 Input reflection coefficient at port 1 and port 2

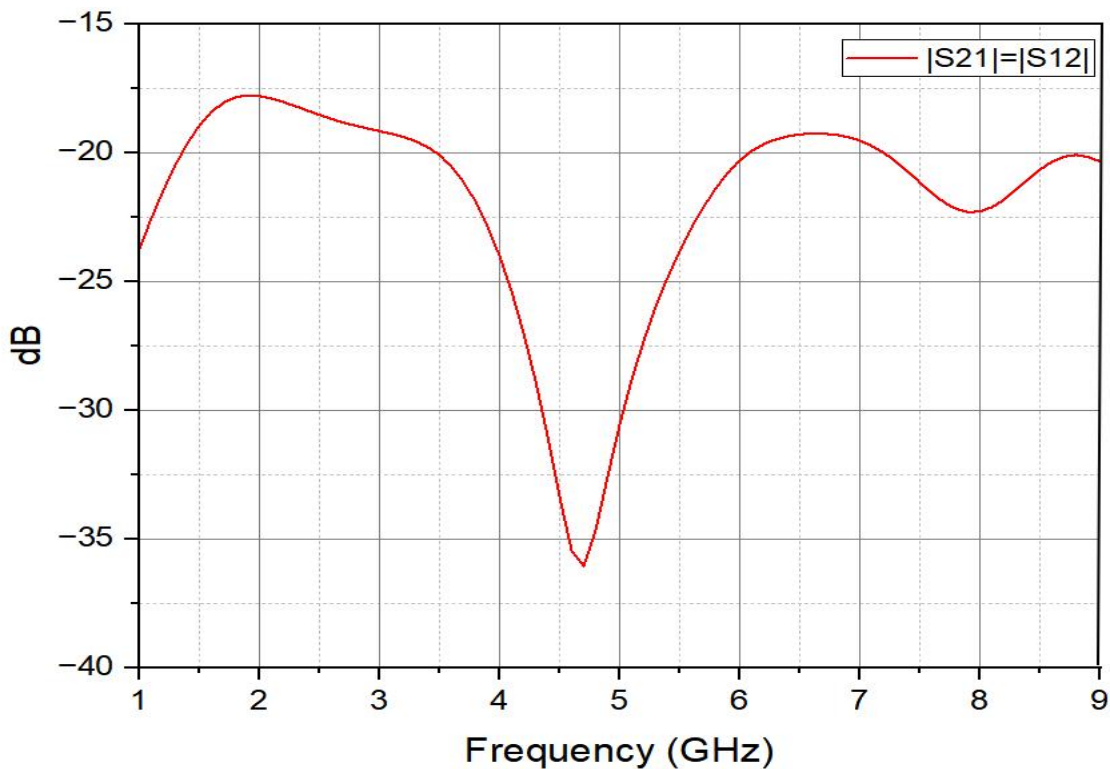


FIGURE 3.13 Transmission coefficient of the Orthogonal MIMO antenna

3.2.2.1 Envelope correlation coefficient (ECC)

From Figure 3.14, it is clearly that the value of ECC is below 0.073.

Furthermore, this value can be considered a good envelope correlation coefficient.

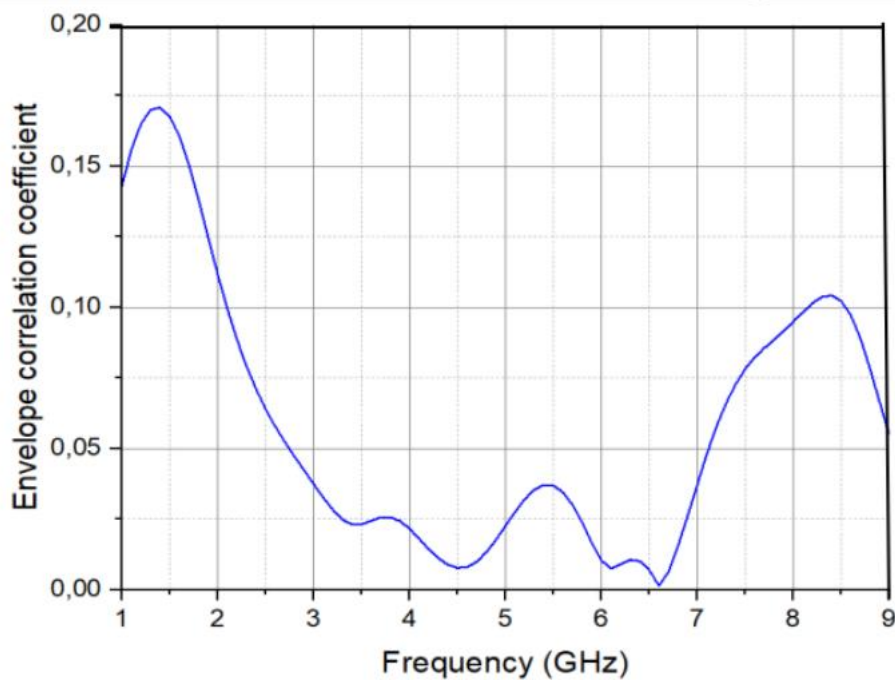


FIGURE 3.14 Envelope Correlation coefficient of 2x1 MIMO system for Orthogonal polarization diversity

3.2.2.2 Diversity Gain

It is shown from Figure 3.15 that the diversity gain of MIMO antenna has values above 9.95 over all frequencies, this value can be considered a good diversity gain.

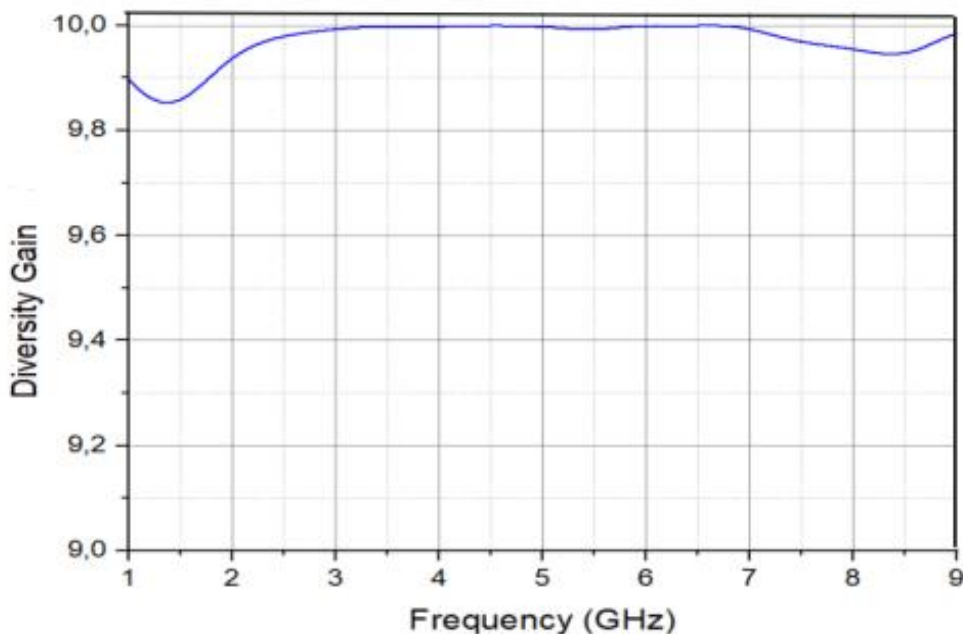


FIGURE 3.15 Diversity Gain of the MIMO antenna with orthogonal configuration

3.2.2.3 Realized Gain

Figure 3.16 represents the orthogonal MIMO antenna’s gain versus frequency. It is shown that gain is enhanced compared to the gain of the reference antenna with a peak gain of 4.5 dBi.

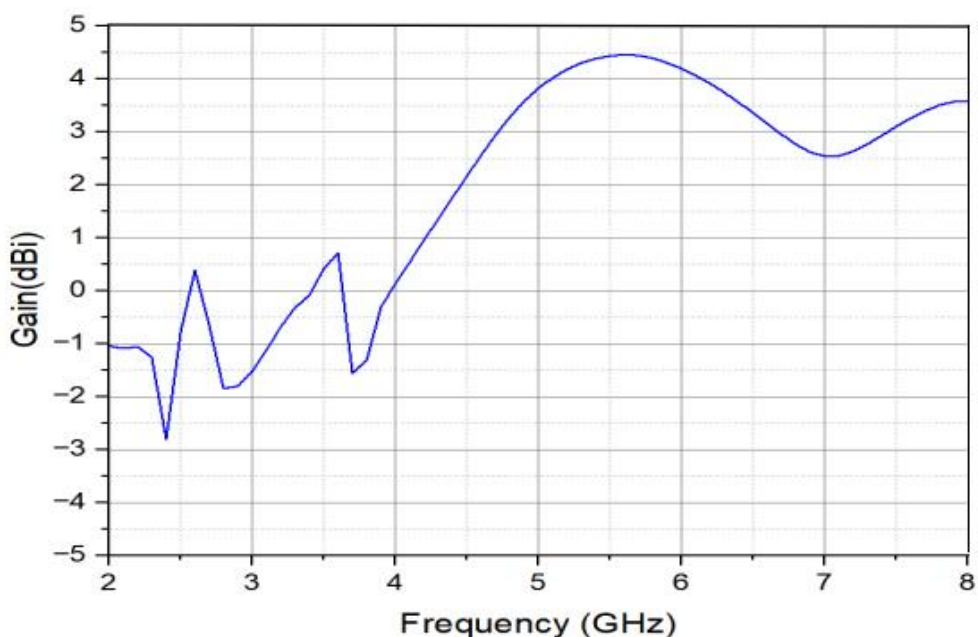


FIGURE 3.16 Gain of MIMO antenna with orthogonal configuration

3.2.2.4 Current Density Distribution

The current density distribution on the two elements when exciting “port 1” at frequencies 3.4 GHz and 6.4 GHz are illustrated in figure 3.17 and figure 3.18 respectively. This figure indicates clearly the current path involved in each of these frequencies. As expected, this path includes the main radiator length at both frequencies.

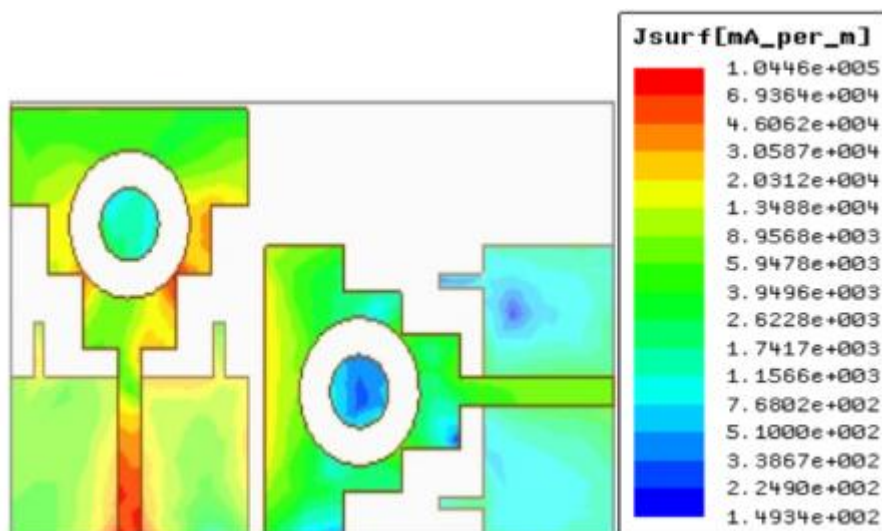


FIGURE 3.17 Current density Distribution of the MIMO antenna with orthogonal configuration at 3.4GHz

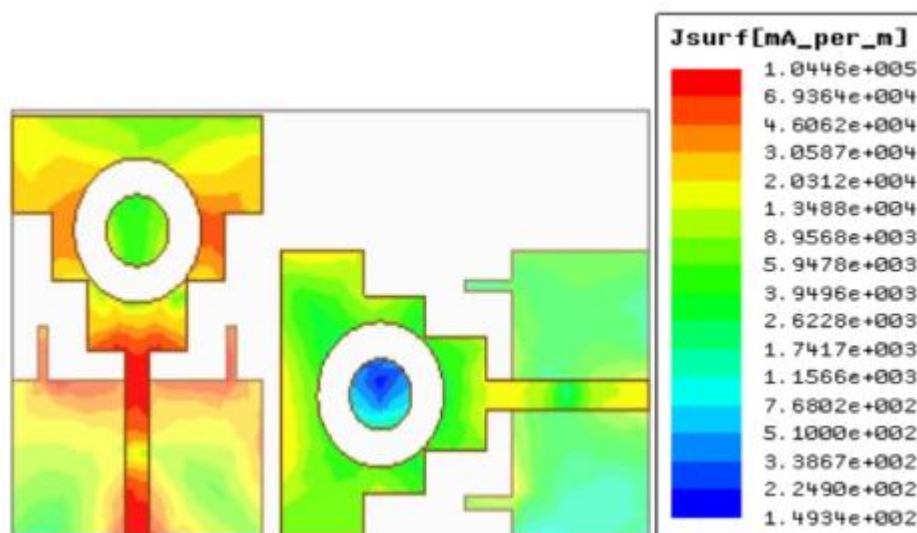


FIGURE 3.18 Current density Distribution of the MIMO antenna with orthogonal configuration at 6.4 GHz

3.2.2.5 Radiation Pattern

The directivity of the two element MIMO antenna is visualized in the 2D polar radiation pattern at port 1 is shown in Figure 3.19.

At $f = 3.4$ GHz, the antenna exhibits a bidirectional pattern in the E-plane with a maximum directivity $D = 0.72$ dB at $\theta = 180^\circ$, and an omnidirectional pattern in the H-plane with a maximum directivity $D = 0$ dB at $\theta = 220^\circ$.

At $f = 6.4$ GHz, the antenna exhibits a bidirectional pattern in the E-plane with a maximum directivity $D = 3.39$ dB at $\theta = 170^\circ$, and an omnidirectional pattern in the H-plane with a maximum directivity $D = 3.31$ dB at $\theta = 180^\circ$.

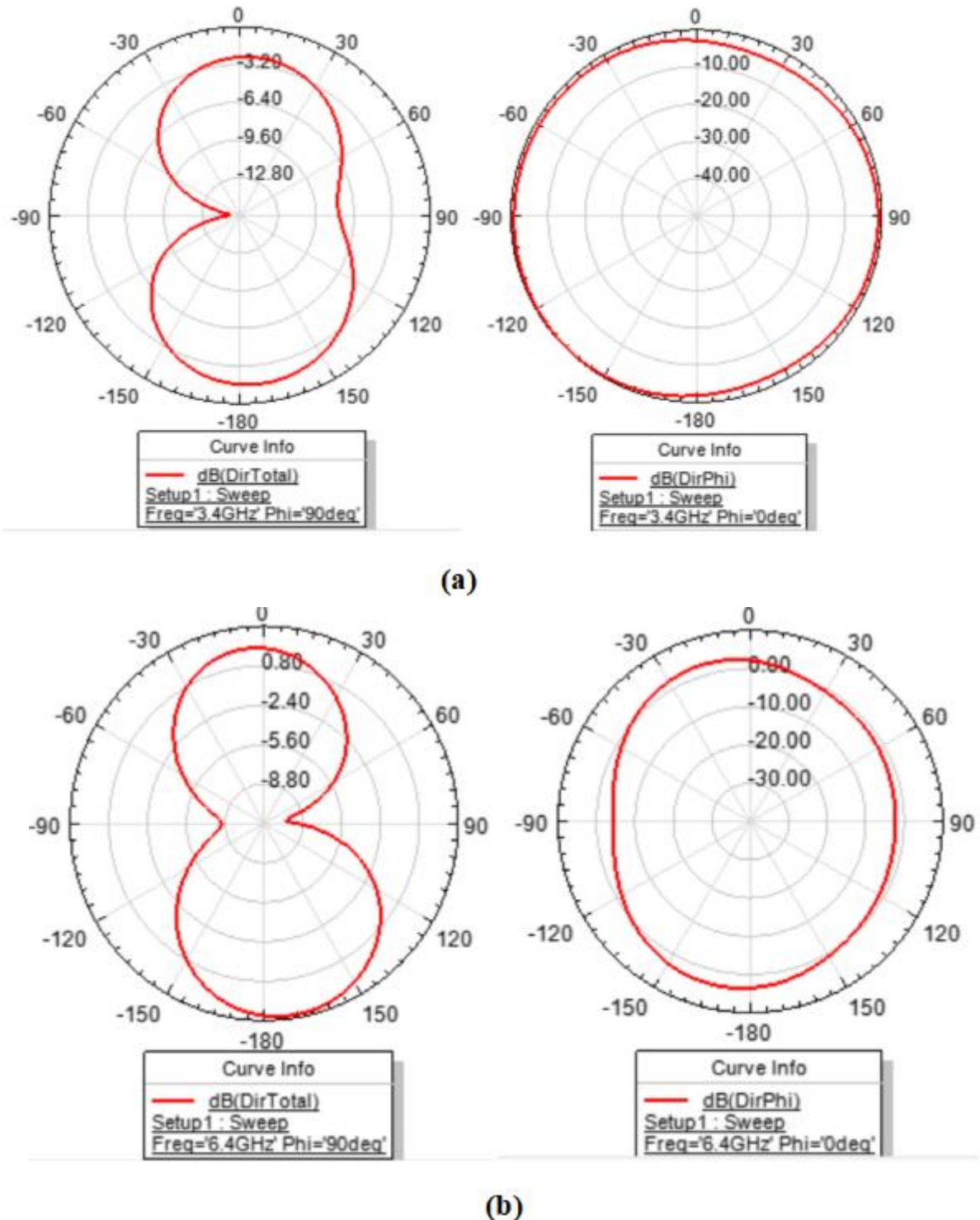


FIGURE 3.19 The 2D radiation pattern of the MIMO antenna with orthogonal configuration, E plane,

and H plane at a) 3.4 GHz b) 6.4 GHz

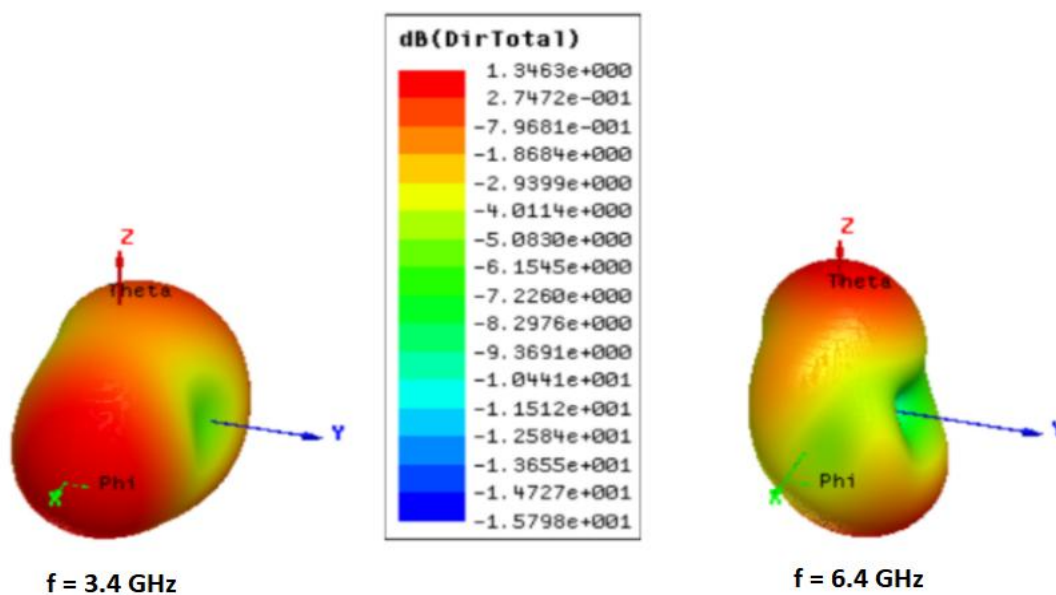


Figure 3.20 The 3D radiation pattern of the MIMO antenna with orthogonal configuration

Table 3.2 summarizes the results in details of the dual element MIMO antenna with orthogonal configuration antenna.

TABLE 3.2: The results of the MIMO antenna with orthogonal configuration

Number of elements	2
Size (mm^3)	$51 \times 30 \times 1.6$
Materials	FR-4 ($\epsilon_r = 4.4$)
Bandwidth of 1 st band (GHz)	1.9
Bandwidth of 2 nd band (GHz)	1.65
Isolation (dB)	-18
ECC	<0.075
DG	>9.95
Peak Gain (dBi)	4.5

3.3 Comparison between parallel and orthogonal configuration

The evaluation results demonstrate that the 2x1 MIMO parallel configuration, with its smaller

size, offers a greater bandwidth than the orthogonal configuration. Despite similar gains and envelope correlation coefficients, the orthogonal configuration provides superior isolation.

3.4 Experimental Verification

Following to the above comparison, the parallel 2×1 MIMO parallel configuration has been selected and, a prototype is fabricated and tested. Figure 3.21 shows the photograph of the fabricated antenna.

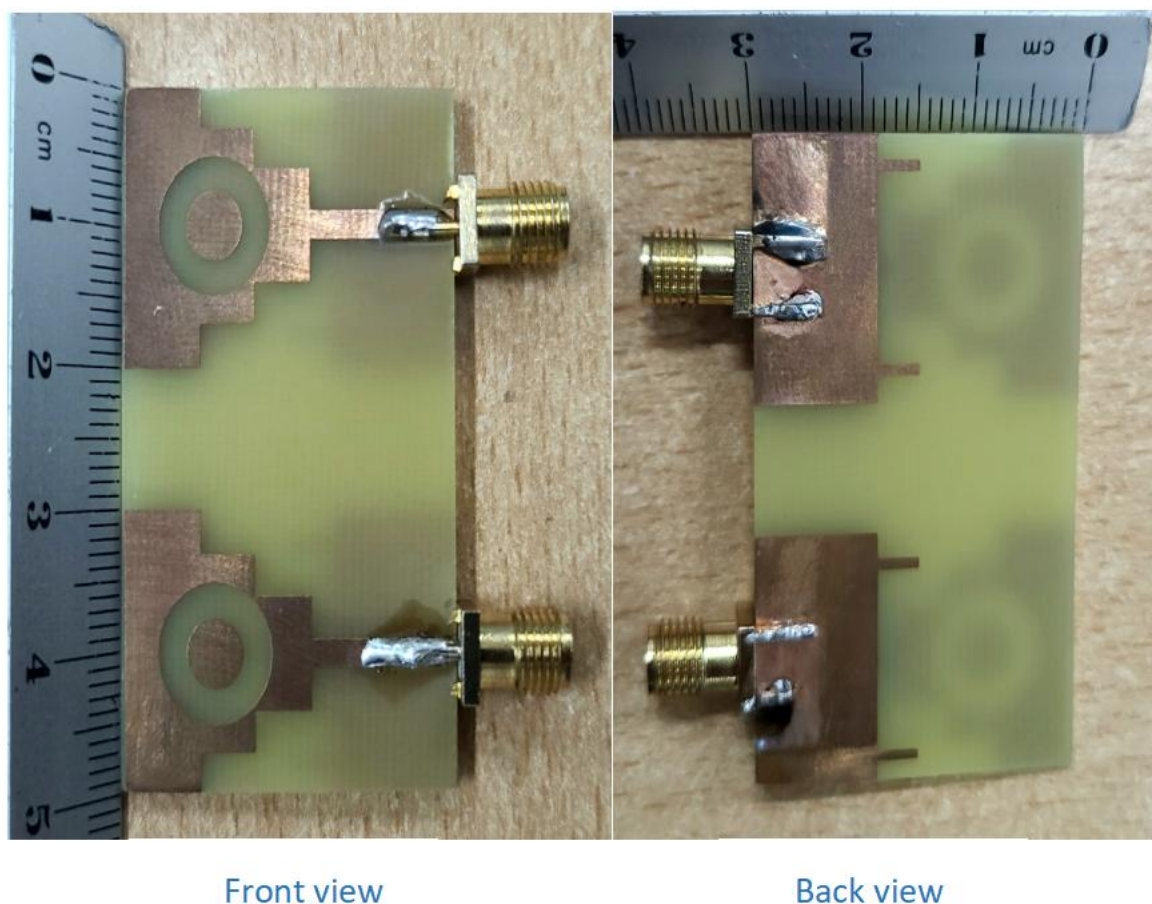


FIGURE 3.21 The front and the back view of 2x1 parallel fabricated MIMO antenna

The measurement of the reflection and transmission coefficients were obtained using VNA. Though the simulated coefficient are equal because of the parallel configuration symmetry thought we observe small difference in the measured coefficients due to experimental conditions. Despite, we observe quite similar profile in both figures.

The Figure 3.22 and Figure 3.23 show the simulated and measured input reflection coefficient at port 1 and port 2 respectively.

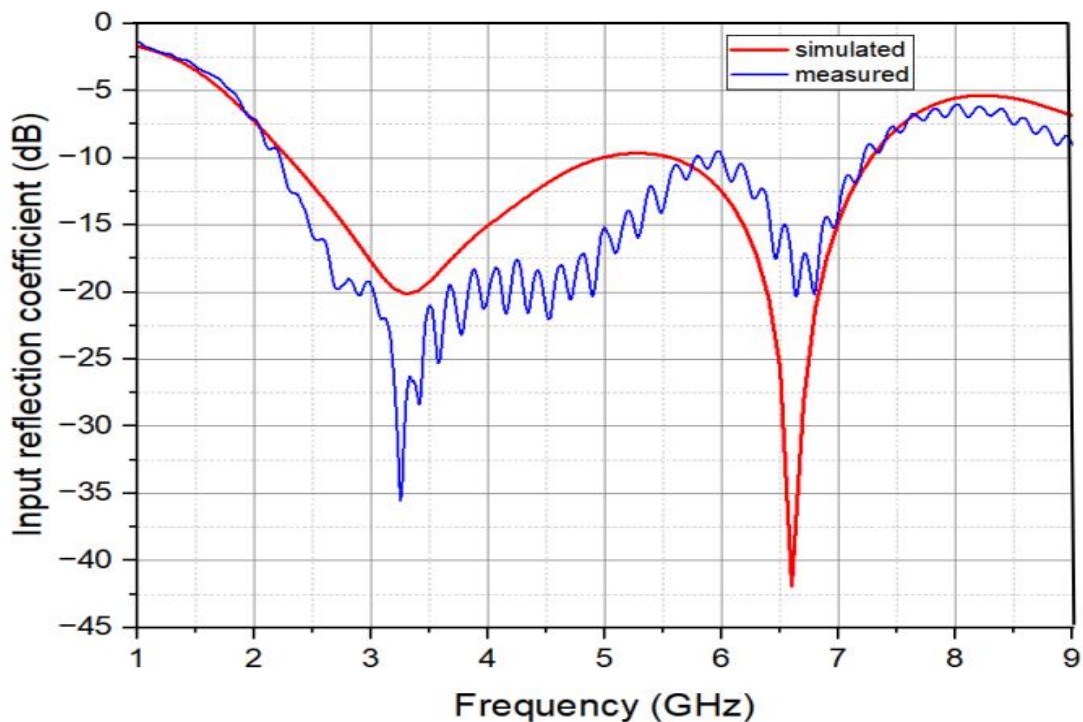


FIGURE 3.22 Input reflection coefficient at port 1

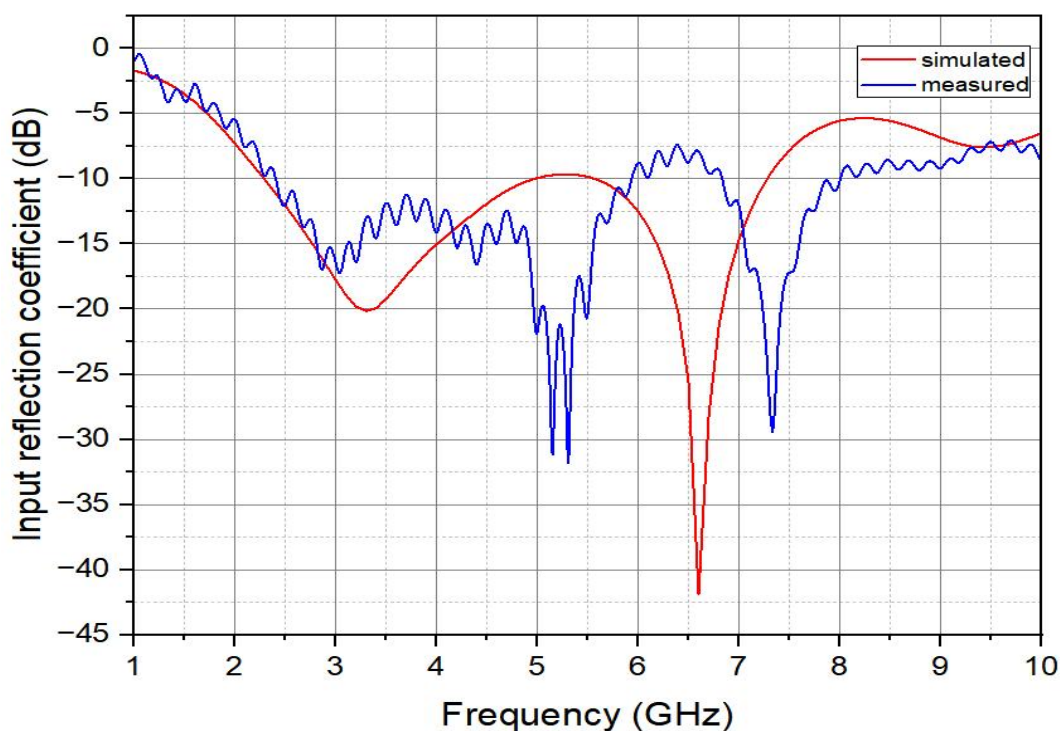


FIGURE 3.23 Input reflection coefficient at port 2

Figure 2.24 shows the transmission coefficient $|S_{21}|$ where we observe relative deviation of the measured value which in some frequency band is slightly greater than -15 dB .Again this is attributed to experimental conditions and fabrication errors (geometrical dimensions, welding...).

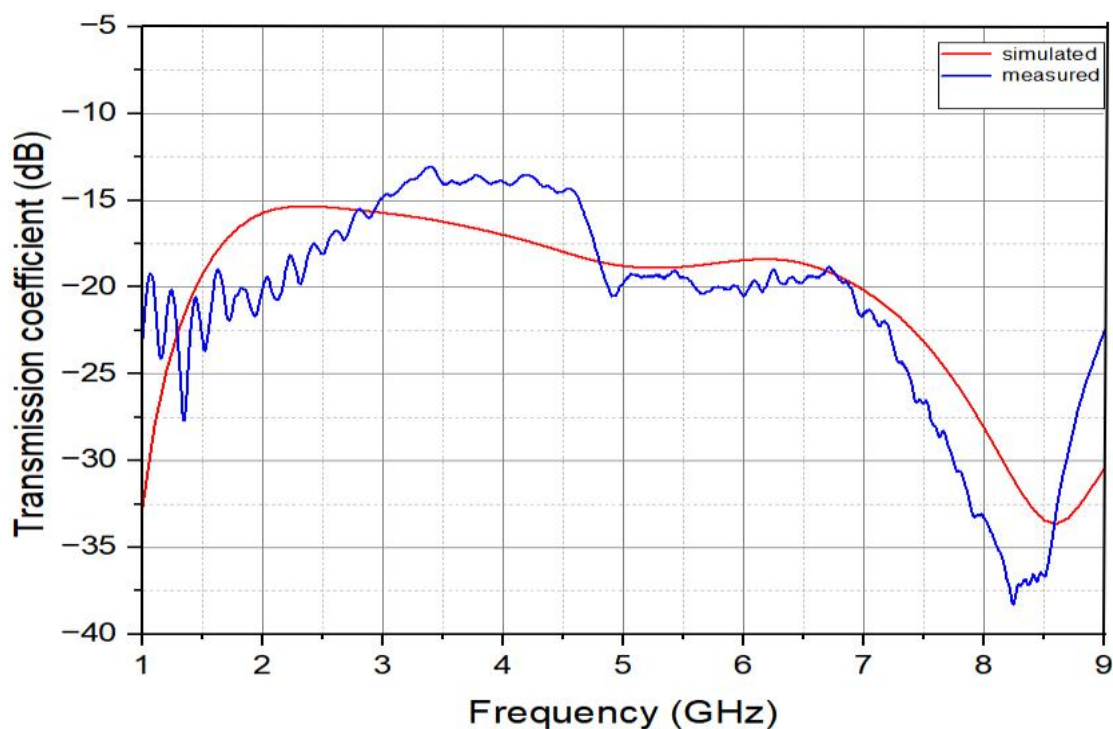


FIGURE 3.24 The transmission coefficient of the simulated and measured MIMO antenna

3.5 Comparison with related works

Table 2.9 shows a comparison between the characteristics of the proposed 2×1 MIMO antenna in parallel configurations with other works aiming similar objectives. This table shows that the proposed antenna exhibits acceptable performance especially dealing with Size, gain, input reflection coefficient and isolation.

TABLE 3.3 Comparison with related works

References	[34]	[35]	[36]	Proposed antenna
Configuration	2×1	2×1	2×2	2×1
Operating band (GHz)	4.5-5	3.26–3.61	3.18-3.9	2.3-5 5.6-7.3
Dimensions (mm^3)	$50 \times 35 \times 1.6$	$85 \times 50 \times 4$	$150 \times 75 \times 1.6$	$50 \times 30 \times 1.6$
Gain (dBi)	1.83	5	4.75	4.5
ECC	<0.07	<0.01	<0.01	<0.075
DG	>9.95	>9.97	>9.9	>9.95
$ S_{11} $ (dB)	-17.18	-16.33	-22	-31.33
Isolation (dB)	-17.2	-18	-11	-18

3.6 Conclusion

Based on the single antenna element developed in the previous chapter, 2×1 MIMO structures in both orthogonal and parallel configuration have been considered in this chapter. Despite the required large distance for isolation between the elements of the parallel configuration, it has been observed that the orthogonal configuration is larger in size.

A prototype of the parallel configuration has been fabricated and tested.

General Conclusion and further work

The goal of this project is to design and study a dual-band microstrip patch antenna, in both single element and 2×1 MIMO configurations, that can be used in wireless communication systems operating in 5G sub-6 GHz applications.

The first part describes the design procedure which has ended up with a monopole staircase ring slotted microstrip patch antenna. The antenna operates in two sub-6 GHz frequency bands dedicated for wireless 5G application, the antenna shows good input reflection coefficient level a quasi-omnidirectional radiation pattern and qualitative radiation efficiency.

After that a parallel and an orthogonal 2×1 MIMO configurations based on the developed single element have been considered and their characteristics involving input reflection coefficient, isolation, envelope correlation coefficient, diversity gain and realized gain were investigated.

Two structures of both configurations achieving MIMO requirement have been obtained.

Furthermore the proposed single element and parallel MIMO configuration have been compared to other referenced similar works, where it is observed that the proposed design achieve acceptable performances. Moreover prototype of these structure have been fabricated and tested.

As further work we suggest:

Extends the number of elements of the MIMO structure.

Using other dielectric material.

Extending the proposed structure for array applications.

References

- [1] P. V. David Tse, *Fundamentals of Wireless Communication*, California, Illinois: Cambridge University Press, 2004.
- [2] E. V. J. JOHN BROWN, "THE PREDICTION OF AERIAL RADIATION PATTERNS FROM NEAR-FIELD," *The Institution of Electrical Engineers* , 1961.
- [3] ., M. A. T. A. T. U. F. A. B. W. Mazhar, "Compact Microstrip Patch Antenna for Ultra-wideband," *PIERS Proceedings*,, 12–15 Aug. 2013.
- [4] D. V. T. Indrasen Singh, "Micro strip Patch Antenna and its Applications: a Survey," *Int J. Comp. Tech. Appl*, vol. Vol 2 (5), pp. 1595-1599, 2011.
- [5] M. E. Ezhilarasan, "A Review on mobile technologies: 3G, 4G and 5G.," IEEE, Vellore, India, 2017.
- [6] M. B. a. L. N. Rafal Przesmycki, "Broadband Microstrip Antenna for 5G Wireless Systems," pp. 1-19, 22 December 2020.
- [7] Mehmet Ciydem and Emre A.Miran, "Dual Polarization Wideband Sub-6 GHz Suspended Patch Antenna for 5G Base Station," *IEEE Antennas and Wireless Propagation Letters*, vol. 19(7), pp. 1142-1146, 2020.
- [8] C. A. Balanis, *ANTENNA THEORY ANALYSIS AND DESIGN*, New Jersey.: John Wiley & Sons, Inc., Hoboken, 2005.
- [9] • R. G. Aakash Bansal, "A review on microstrip patch antenna and feeding techniques," *Int. j. inf. tecnol*, vol. 12, p. 149–154, 28 February 2018.
- [10]A. a. R. V. Kumar, "Design Analysis of Different Types of Feed to Microstrip Patch Antenna," *IRE Journals*, vol. 1, no. 6, DEC 2017.

- [11]A. a. R. G. Bansal, "A review on microstrip patch antenna and feeding techniques," *International Journal of Information Technology*, vol. 12, pp. 149-154, 2020.
- [12]S. S. S. V. P. a. B. N. Bisht, "Study the various feeding techniques of microstrip antenna using design and simulation using CST microwave studio," *International Journal of Emerging Technology and Advanced Engineering* , vol. 4, no. 9, pp. 318-324., 2014.
- [13]S. S. S. P. V. & N. B. Bisht, "Study The Various Feeding Techniques of Microstrip Antenna," *International Journal of Emerging Technology and Advanced Engineering*, vol. 4, no. 9, pp. 318-324, September 2014.
- [14]A. AZRAR, " Antennas course for master telecommunication option".
- [15]C.-T. a. C. P. Tai, "An approximate formula for calculating the directivity of an antenna," *IEEE Transactions on Antennas and Propagation*, vol. 24, no. 2, pp. 235-236., 1976.
- [16]W. L. Stutzman, "Estimating directivity and gain of antennas," *IEEE Antennas and Propagation Magazine*, vol. 40, no. 4, pp. 7-11., 1998.
- [17]S. S. A. L. C. P. T. R. S. C. D. a. W.-S. L. Ankan, "A planar monopole antenna array with partial ground plane and slots for sub-6 GHz wireless applications," *IEEE Wireless Antenna and Microwave Symposium (WAMS)*, pp. 1-5, 5 Jun 2022.
- [18]R. P. L. G. C. I. Y. a. G. P. Dangi, "Study and investigation on 5G technology: A systematic review," *Sensors*, vol. 22, no. 1, p. 26, 2022.
- [19]C. J. E. M. M. B. M. a. C. R. Hausl, "Mobile network testing of 5G NR FR1 and FR2 networks: Challenges and solutions," in *16th European Conference on Antennas and Propagation (EuCAP)*, Rohde & Schwarz, Munich, Germany, 2022.
- [20]D. M. S. V. S. P. P. K. a. T. A. John, "Flexible antennas for a Sub-6 GHz 5G band: a comprehensive review.," *Sensors* , vol. 22, no. 19, p. 7615, 2022.

- [21]S. W. Minehane, "Spectrum Requirements for digital transformation," in *International advocacy & consultancy*, JAKARTA, 6 February 2020.
- [22]T. O. a. P. K. Olawoye, "A high gain antenna with DGS for sub-6 GHz 5G communications," *Advanced Electromagnetics*, vol. 11, no. 1, pp. 41-50, 2022.
- [23]A. R. M. a. P. K. Kapoor, "Compact wideband-printed antenna for sub-6 GHz fifth-generation applications," *International Journal on Smart Sensing and Intelligent Systems*, vol. 13, no. 1, pp. 1-10, 2020.
- [24]R. R. S. A. C. a. S. K. M. Kumar, "A compact microstrip feedline printed antenna with perturbed partial ground plane for UWB applications," *International Journal of RF and Microwave Computer-Aided Engineering*, vol. 31, no. 9, 2021.
- [25]P. J. S. K. a. C. S. P. Pradeep, "Design of a Novel Compact L-slotted Monopole Antenna for 5G Applications in sub-6 GHz Band," in *International Conference on Electronics and Sustainable Communication Systems (ICESC)*, 2022.
- [26]I. Mujahidin, "Directional 1900 MHz Square Patch Ring Slot Microstrip Antenna For WCDMA," *Journal of Electrical Engineering, Mechatronic and Computer Science*, vol. 21, no. 11, pp. 42-45, 2015.
- [27]M. F. A. M. H. A. E. a. W. S. Sree, "Dual Band Patch Antenna Based on Letter Slotted DGS for 5G Sub-6GHz Application," *In Journal of Physics: Conference Series*, 2021.
- [28]I. M. A. A. Z. M. F. A. J. K. a. S. A. Rafiqul, "Design of microstrip patch antenna using slotted partial ground and addition of stairs and stubs for UWB application," *Cyber Journals: Multidisciplinary Journals in Science and Technology, Journal of Selected Areas in Telecommunications (JSAT)* , pp. 1-8, 2012.
- [29]D. K. Naji, "Compact design of dual-band fractal ring antenna for WiMAX and WLAN Applications," *International Journal of Electromagnetics and Applications*, vol. 6, no. 2, pp.

42-50, 2016.

- [30]M. F. A. M. M. A. A. D. E. F. D. B. L. a. M. F. A. S. Nakmouche, "Development of H-slotted DGS based dual band antenna using ANN for 5G applications," in *15th European Conference on Antennas and Propagation (EuCAP)*, 2021.
- [31]J. D. K. C. a. R. K. C. Kukreja, "CPW fed miniaturized dual-band short-ended metamaterial antenna using modified split-ring resonator for wireless application," *International Journal of RF and Microwave Computer-Aided Engineering*, vol. 27, no. 8, 2017.
- [32]X. S. Z. a. Q. L. Chen, "A review of mutual coupling in MIMO systems," *Ieee Access*, vol. 6, pp. 24706-24719, 2018.
- [33]S. L. B. a. M. M. Kolangiammal, "A Compact Planar Monopole UWB MIMO Antenna for Short-Range Indoor Applications," *Sensors*, vol. 23, no. 9, p. 4225, 2023.
- [34]O. P. ., E. O. A. ., Z. S. B. 3. R. 3. a. A. A.-A. 2.-E. 5. M. A. f. S.-6. G. A.]Arpan Desai, "Transparent 2-element 5G MIMO antenna for sub-6 GHz applications," *Electronics* , vol. 11, no. 2, p. p.251, 2022.
- [35]N. a. D. K. Sharma, "A compact two element U shaped MIMO planar inverted-F antenna (PIFA) for 4G LTE mobile devices," in *Fifth International Conference on Parallel, Distributed and Grid Computing (PDGC)*, 2018.
- [36]U. S. K. M. M. A. S. H. K. S. M. A. S. I. S. M. A. a. M. D. Rafique, "Uni-planar MIMO antenna for sub-6 GHz 5G mobile phone applications," *Applied Sciences*, vol. 12, no. 8, p. p.3746, 2022.